THE UNIVERSITY OF MICHIGAN

COLLEGE OF ENGINEERING

Department of Nuclear Engineering
Laboratory for Fluid Flow and Heat Transport Phenomena

Technical Report No. 03424-20

FURTHER CAVITATION DAMAGE CHARACTERISTICS IN A CAVITATING VENTURI USING WATER AND MERCURY AS TEST FLUIDS

M. J. Robinson
F. G. Hammitt
J. F. Lafferty
R. Garcia

Financial Support Provided by:

National Aeronautics and Space Administration
Grant No. NsG-39-60

September, 1966

ACKNOWLEDGMENTS

The authors would like to acknowledge the assistance of Osman S. M. Ahmed, doctoral candidate, Department of Nuclear Engineering, for conducting a portion of the tests described herein; Joseph Lawrence and Thomas MacDonald of the Department of Chemical and Metallurgical Engineering at this University, for their work on the metallograph, and the former of these for his work with the electron microscope; also Professor Clarence A. Siebert of the same department for supervising and interpreting this work. Financial support for the investigation was furnished under NASA Grant No. NsG-39-60.

ABSTRACT

During the course of the continuing investigation into many aspects of cavitation damage characteristics and cavitating flow regimes in this laboratory over the past several years, several miscellaneous topics have been investigated in a cursory manner, and were not documented in a suitable fashion, since they did not fit well into one of the previous reports. This report attempts to document these various topics, preserve them for the record, and draw any pertinent conclusions from them. Included are various previously unpublished cross-sectional photomicrographs of materials that have been damaged in the cavitation damage programs; the results of an investigation into the handling procedures for the samples; the results of an investigation into the presumed corrosion and/or erosion conditions in the systems, where the samples were exposed to the same test conditions as the cavitated specimens but without cavitation present; some preliminary attempts at electron microscope recordings and photographs of the cavitated surfaces; and finally the results of some computer analyses of the venturi cavitation damage data, which show the relevancy of a simple single-property correlation, previously derived from the vibratory test data of this laboratory, to the mercury venturi data.

TABLE OF CONTENTS

LIST OF TABLES

LIST OF FIGURES

CHAPTER I

INTRODUCTION

This laboratory has conducted many investigations into the damage and flow regimes of cavitating systems over the past few years. During this time many complete reports have been issued[1,2,3,4,etc.] covering completed segments and portions of several phases of these investigations. However, there have been many preliminary attempts to try to understand and find out more about the damage and flow characteristics, that have been left in various stages of incompleteness, due to either lack of funding, lack of properly trained personnel, lack of time, or to the fact that it was not economically feasible to complete the analysis at the present time. Since many of these analyses were done by students at the University, and since many of these students have since departed, it becomes necessary to document, whether complete or not, these analyses, so that they could be continued and finished at a later date if it is deemed desirable.

There have been many metallographic examinations made of the various materials tested during the investigation and for the sake of completeness these have covered complete series of cavitation tests on selected materials. The copper-zinc-nickel material set that was tested

in several heat treats[3,4,5] has been examined in detail with cross-sectional photographs and the results are reported herein. In addition several miscellaneous pitting formations were observed on plexiglas samples that had been cavitated in the water facility, and these are also included.

Throughout the investigation it has been realized that the total damage in a relatively low intensity cavitation field such as is provided by the cavitating venturis which were used cannot be entirely ascribed to mechanical damage since some degree of corrosion and/or erosion is undoubtedly also active on the test specimens. Although materials have been selected for the cavitation tests that were as chemically compatible with the test fluids as possible, it was deemed desirable to examine the effect of corrosion and erosion, and also the necessary physical handling of the specimens, in the absence of cavitation. Therefore, a set of specimens of one of the materials most likely to be affected by these phenomena, namely the copper-zinc-nickel series, was selected to be put through the identical series of steps as the normal test specimens, with the exception that no cavitation was present on the specimens during the procedure. Thus, it was hoped to delineate between the combined cavitation-erosion-corrosion-handling damage and that incurred in the absence of cavitation. In similar fashion it was decided to conduct a continuous 100 hour test of a set of specimens to investigate any possible differences between this procedure, and that usually followed of removing the specimens approximately 10 times for examination during the 100 hour tests. The results of these investigations are reported herein.

A very preliminary attempt has been made to obtain more information on the very detailed size and shape of the individual cavitation craters on test specimen surfaces using electron photomicroscopic procedures. The results of this analysis and recommended future considerations in this regard are included herein.

Finally, in continuation of past attempts to obtain a correlation between the cavitation damage sustained by the specimens and the mechanical properties of these materials,[3,4] a property of the materials not previously considered, i.e., namely the ultimate resilience,[5] has been analyzed with the computer regression analysis[3,4,5] used in the past to show the degree or lack of correlation between these above variables for the venturi damage data from the water and mercury facilities. A similar successful correlation has already been reported for vibratory cavitation damage tests.[5]

CHAPTER II

DESCRIPTION OF FACILITY

The two closed-loop facilities used for the current investigations have been described in many past reports,[1,2,etc.] and a complete description is available in the open literature.[6] Therefore, the following description will be very brief.

The two cavitating venturi, closed-loop tunnels, using water and mercury as test fluid, are shown in Figures 1 and 2, respectively. The venturis used for test specimen insertion are shown in Figures 3 and 4, respectively, and the actual test specimen design is shown in Figure 5. It is possible to obtain velocities between 65 and 200 ft./sec. and temperatures from about 50°F to 150°F for several degrees of cavitation in water, and velocities between 25 and 50 ft./sec. and temperatures between about 50°F and 500°F for several degrees of cavitation in mercury. The "degrees of cavitation" as used herein are defined in the appendix.

CHAPTER III

EXPERIMENTAL PROGRAMS

The results of the various relatively unrelated but previously unreported sub-investigations listed in the Introduction are presented in this section.

A. Photomicrographic Cross Sections of Materials From Venturi Damage Tests

After the cavitation damage investigations had been completed on most materials to the desired duration, and after all nondestructive data had been taken from them, it was decided to section the materials in a direction perpendicular to both the polished surface, Figure 5, and to the direction of fluid flow on the surface during the tests. This was done in order to obtain more detailed information on the depth and profile of the pits, and to examine whether damage had been done to the grains immediately beneath the surface of the materials. Figures 6 through 11 show typical cross sections for the copper-zinc alloy, Figures 12 through 17 for the copper, Figures 18 through 23 for the copper-nickel, and Figures 24 through 29 for the nickel. In each case the top photomicrograph is of an unetched specimen, while the lower photomicrograph is of an etched specimen to show grain boundaries. All of these

materials had been previously exposed to the cavitation environment in the water facility at a throat velocity of 200 ft./sec., a temperature of 80°F, and "standard cavitation," for a duration of 100 hours.

A cavitation test specimen representing each of the three heat-treat states of these alloys was sectioned. Photomicrographs were then made of a region including the surface from the center portion of the specimen and one showing the corner. An unetched and an etched photomicrograph were taken of each area, although the same exact location was not covered in each instance. Figure 6 shows a typical blunting of the edge of a specimen, which is thought to be due to handling and does not represent any weight loss. In the following photomicrographs, only slight damage can be seen although the magnification is about 250X. This is due to the fact that the pits are typically on the order of 0.05 mils in diameter, with a depth to diameter ratio of approximately 0.03.[4] Therefore, at this magnification, a typical pit would be only about 0.4 mils deep at the scale of the photograph and about 0.0125 inches across, so that it would be difficult to see. However, a close examination of most of these cross-section photomicrographs does show such pitting (Figures 6, 7, 9, etc.), and previously reported photomicrographs of the surface itself show substantial pitting on similar specimens.[4] Figure 30 is typical, also showing proficorder traces of the surface. Figure 9, for example, also shows considerable distortion of the surface layer which has been somewhat cold-worked by the cavitation attack. This often results in a measurable increase in surface hardness as verified in an earlier report.[4] No preferential attack along the grain

boundaries has been noted, as seen most clearly in Figure 17, for the high heat-treat pure copper. The bump appearing on the surface in Figure 19 is believed due to improper handling of the specimen. There is little else to be concluded from the rest of these photomicrographs except verification of the points already made. However, they do record the grain structure of the cavitated specimens, the weight loss of which has been reported elsewhere,[3,4] and thus have been included here.

A peculiar form of damage was noted on the nickel samples tested in mercury.[3] Since it was thought that this was due to some form of corrosion of the surface by the mercury, one of these samples was sectioned. Figures 31 and 32 are sections at 1000X of nickel specimens tested in mercury. It is noted that there is indeed much surface attack to a depth of about 0.1 mils, although it is not obviously due primarily to corrosion. The damage could have initially started by mechanical pitting, destroying any protective film that might have formed, thus exposing fresh metal to the mercury. Then, succeeding exposure to the mercury might have resulted in solution of nickel from the surface or other chemical attack in these local areas of previous mechanical damage. Thus, as is often the case, the combined action of corrosion and cavitation may be much more severe than either taken singly. There is no evidence in the etched photos of a corrosion layer on the surface, even in the obviously damaged areas. However, as pointed out above, the surface could have been cleaned of these corrosion products as fast as they were generated by the intense action of the cavitation regime. There is also no evidence of intergranular corrosion. In some areas it does appear

that some grains have undergone more damage than others. Figures 33 and 34 are similar photomicrographs of the surface of stainless steel tested in mercury. Here it is noted that there are not as deep pits as in the nickel, and the damage appears to be less severe. Again, there is no indication of intergranular corrosion.

B. Pitting in Plexiglas

In past reports it has been noted that plexiglas behaves quite differently from most materials in the water facility. While in the mercury system the plexiglas test specimens and venturi are severely damaged, there was almost a complete lack of damage to both in the water system, even after very long exposures. In fact, the same venturis were used for almost the entire water test series, and thus were submitted to literally thousands of hours of cavitation without incurring visible damage. Somewhat similar results are also reported from Pennsylvania State University.[7] However, a high-magnification examination of one of the plexiglas test specimens from the water loop indicates the peculiar pitting pattern shown in Figures 35, 36, and 37. These pits are very similar in appearance to pits produced by Bowden and Brunton[8] in plexiglas by high velocity liquid drop impact. Thus, the hypothesis is supported that the damage from the individual imploding cavitation bubbles is caused by a very high-speed microjet of liquid. Comparing the diameter of the Bowden and Brunton craters with those presently obtained and assuming as a rough estimate that the ratio of jet to pit diameter is relatively constant, the diameter of the microjet in the present

cavitation case would be about 0.25 mils. Figures 35, 36, and 37 show the same pits photographed at the increasingly larger magnifications of 500X, 1000X, and 2000X, respectively, so that more detail of the individual pits can be obtained. The photomicrographs appear to show craters with raised approximately symmetrical rims, and a somewhat off-center deeper central pit. The actual rim diameter is about 0.5 mils. The area immediately surrounding the central pit, presumably created by the impingement of the microjet, appears undamaged out to the rim, which is apparently divided into many small segments. No precise detailed mechanism to explain the detailed pit shape is available. However, it does seem more consistent with the microjet hypothesis than with the impingement of shock waves from a collapse point off the surface as required by the classical Rayleigh collapse hypothesis.

It would be desirable to obtain sections through these pits to determine the actual surface displacement and possible subsurface failures, as observed by Bowden and Brunton.[8]

C. Zero Cavitation and Continuous 100 Hour Runs

Several materials have been run in both the water and the mercury facilities under the same velocity and temperature conditions as the normal cavitation damage specimens; however, under a zero cavitation condition, i.e., the loop pressure was raised sufficiently to suppress cavitation, but the usual velocity and temperature conditions were maintained. In both facilities there has been no measurable weight loss for these "zero cavitation" specimens.

Three specimens each of plexiglas, stainless steel, and carbon steel were cavitated in the water facility for continuous durations of 100 hours to determine whether the usual handling procedures themselves, involving the removal of the specimens at frequent intervals for inspections, weighings, pit countings, etc., contributed significantly to the measured weight loss. For the plexiglas specimens there was no noticeable or detectable damage as was the case for the normal specimens of plexiglas tested. For the stainless steel specimens the damage for the continuous run was the same as that for the normal runs within the usual experimental scatter between specimens, indicating that the handling procedures did not significantly affect the damage. The carbon steel specimens showed very large weight losses and visible evidence of corrosion after the continuous run, as they had for the normal runs, indicating that they should not be included in the mechanical properties correlations, due to the large effect of corrosion. They had, in fact, been so excluded.[3,4] The carbon steel specimens tested in the usual fashion lost even more weight than those run continuously. This may be attributable to the cleaning of the specimens for weighing and pit counting in the ordinary runs which obviously removes some corrosion products, and exposes fresh surface to additional corrosion.

D. Handling and Storing Procedure Checkout

In many cases, the weight loss incurred by test specimens in the venturi facility was quite small. Also, the surfaces of some of the copper-zinc-nickel alloys became somewhat discolored after extensive

testing, perhaps indicating substantial chemical attack which might or might not be related to the cavitation. Thus, it was desirable to determine how much of the measured weight loss and observed pitting might be due to conditions in the test procedure (handling, static corrosion, etc.) other than cavitation and high velocity erosion, corrosion, etc. Thus, a set of specimens of various materials was put through the same physical steps as a normal set of specimens following the standard procedures. The only difference was that these specimens were not exposed to a flowing and/or cavitating liquid. They were weighed, pit counted, inserted and removed from the loop, and left in static water in the loop, all for the same number of times and durations used for a standard damage set. For a 100 hour test, the inspection procedure is normally performed at 1, 4, 10, 20, 30, 40, 50, 75, and 100 hour total exposure times in the test. Table 1 lists the results in terms of weight loss and pit counts that occurred on these samples as well as typical cavitated samples. It will be seen that the handling procedures do not contribute significantly to the weight loss. However, the number of very large pits (VVL and VL categories as defined in Table 1) are of the same order of magnitude for cavitated and noncavitated samples. Hence, apparently many of these pits do result from handling, and not from the cavitation bubbles.

E. Electron Microscope Photomicrographs

An initial attempt was made to photograph cavitation damage on type 304 stainless steel with an electron microscope. The specimen used

TABLE 1

SUMMATION OF DATA ON HANDLING PROCEDURE SPECIMEN SET

Specimen Number	Weight Loss(gm)	Pit Count Increase VVL	VL	L	S	Material
Handling Set (100 hour procedure)						
147-cn	+0.00001	7	7	2	2	copper-nickel HHT
148-cn	-0.00004	4	6	0	5	copper-nickel HHT
219-cu	-0.00007	1	0	-1	-2	OFHC copper HHT
220-cu	+0.00008	0	0	6	0	OFHC copper HHT
190-3	-0.00017	3	5	10	3	304 Stainless Steel
191-3	-0.00002	1	0	0	1	304 Stainless Steel
4-4	-0.00015	2	0	3	4	2024 Aluminum
5-4	-0.00016	6	5	5	1	2024 Aluminum
25-F	-0.00010	3	4	5	-2	Tenelon
Normal Set (100 hour procedure)						
220-cn	-0.00073	4	8	21	350	copper-nickel HHT
221-cn	-0.00065	5	7	17	179	copper-nickel HHT
168-cu	-0.00283	uncountable				OFHC copper HHT
169-cu	-0.00375	uncountable				OFHC copper HHT
148-3	-0.00029	2	8	36	871	304 Stainless Steel
149-3	-0.00028	4	9	25	1023	304 Stainless Steel
76-2	-0.05149	uncountable				2024 Aluminum
77-2	-0.05332	uncountable				2024 Aluminum
1-F	-0.00015	0	3	20	294	Tenelon

Pit Size Code

S: 0.4 mils < pit diameter < 1.0 mils
L: 1.0 mils < pit diameter < 2.4 mils
VL: 2.4 mils < pit diameter < 4.8 mils
VVL: 4.8 mils < pit diameter < 9.6 mils

had been subjected to a cavitation field in mercury for one hour with an ultrasonic vibratory horn device, which has been used extensively in this laboratory for cavitation damage studies.[5,etc.] Initially the specimen surface was of "as machined" texture (not ground or lapped). While the detail obtained (Figures 38, 39, 40, and 41) is very good, it is difficult to interpret. This difficulty arises because of the very high magnification of 60,000X, and due to the present lack of any reference photographs of similar undamaged surfaces.

Now that it has been demonstrated by this initial "feasibility test" that good detail can be obtained with such a large magnification, a succeeding investigation would be desirable, where the surface would be carefully polished before the test, standard photomicrographs taken before exposure at several magnifications, and also after exposure of the same region and at the same magnifications. The succession of photomicrographs at different magnifications should include exactly the same area, and the larger magnification photos should cover an area which would be a portion of that covered by the smaller magnification photos. Thus, a precise area can be followed through the different magnifications, and a determination of exactly what portion of the surface is shown by the high magnification photomicrograph would be possible. At the largest magnification used (60,000X), a typical cavitation pit, having a diameter of 0.05 mils in the venturi tests,[3] would be magnified to a photographic size of 3 inches. This should give very good detail of the surface distortion due to the pitting, and should shed more light on the probable bubble collapse and corresponding damage mechanisms.

F. Ultimate Resilience Correlations

Many correlations have been attempted in this laboratory, using a least mean square fit regression analysis, between material mechanical properties, fluid properties, and cavitation damage in terms of rate of volume loss per unit exposed area, i.e., mean depth of penetration rate or MDPR, using both the venturi facilities[3,4] and an ultrasonic vibrating horn.[5,etc.] In the case of the vibrating horn it was found that the best relatively simple overall correlation for MDPR, for fixed fluid and test parameters, was obtained in terms of the ultimate resilience,[9] defined as follows:

$$UR = 1/2 \frac{(TBS)^2}{E}$$

where:

TBS = true breaking stress

E = elastic modulus

Under these conditions it was found that MDPR was inversely proportional to the square root of ultimate resilience. These tests included data gathered in water, mercury, and the molten metals: lead-bismuth alloy and lithium.

An optimum correlation has, therefore, been obtained using the least mean square fit regression analysis previously discussed[3] for both the mercury and water venturi data considered separately in terms of the square root of ultimate resilience. Table 2 shows that this property alone correlates the mercury data very well, in fact better than any single property correlation previously obtained for this data and

TABLE 2

CORRELATIONS OF WATER AND MERCURY VENTURI DATA

Property	Correlating Relation	CD**	Std. Error
A. Single Property Correlation[3] of Mercury Venturi 50 Hour Data			
1. Ultimate Resilience (UR)	$MDP^{*} = 0.034 - 0.879\times10^{-3}(UR)^{1/2}$	0.878	0.0073
2. True Breaking Stress (TBS)	$MDP = 0.025 - 0.63\times10^{-12}(TBS)^{2}$	0.850	0.0080
3. Engineering Strain Energy (ESE)	$MDP = 0.028 - 0.54\times10^{-6}(ESE)$	0.830	0.0090
4. Percent Elongation (ELON)	$MDP = 0.029 - 0.24\times10^{-1}(ELON)^{1/2}$	0.820	0.0090
5. True Strain Energy (TSE)	$MDP = 0.008 + 0.24\times10^{12}(TSE)^{-3}$	0.800	0.0090
B. Single Property Correlation[3] of Water Venturi 100 Hour Data			
1. Acoustic Impedance Ratio (AI)	$MDP^{*} = 0.095 + 4.75(AI)^{3} - 0.239(AI)^{-1/3}$	0.970	0.107
2. Ultimate Resilience (UR)	$MDP = 0.106 + 36.40(UR)^{-1/2}$	0.101	1.200

*Total mean depth of penetration incurred during test.

**Coefficient of Determination.

including most of the standard mechanical properties. The correlation with the five best of these other properties is shown in descending order based on coefficient of determination in Table 2. However, ultimate resilience does not show a significant correlation with the water data (Table 2).

It is encouraging to note that the correlation is successful for the mercury data which is believed to be considerably more accurate than the water data, since the weight losses were large, so that there was little error due to weighing accuracy. The lack of correlation for the water data is believed partly due to weighing errors, since the weight losses are small. Also, it is believed that corrosive influences are much more important in the water data.

It was not possible to include the fluid density along with the ultimate resilience in the correlation, as was done for the vibrating horn data, since the fluid velocity cannot be made identical for the two fluids due to loop limitations.

CHAPTER IV

RESULTS AND CONCLUSIONS

The major conclusions from the miscellaneous investigations follow.

a) There is no visible corrosion on the surfaces of any of the test specimens that have been sectioned from the water system tests. There was, however, corrosion on the carbon steel specimens (which were not sectioned). Also, no corrosion was evident for the specimens from the mercury tests. These conclusions are strengthened by the "zero cavitation" tests where it was found that only relatively negligible damage occurred.

b) The usual pits observed on plexiglas specimens from the water system tests support the liquid jet damage hypothesis as opposed to the shock wave hypothesis.

c) An investigation of handling and storing procedures indicated that negligible weight loss was so incurred. It appeared, however, that the majority of the very large pits that have been observed on the test specimen surfaces are caused by the handling procedure.

d) An electron microscope was used to obtain pictures of excellent clarity of a damaged surface at 60,000X. It is believed the

procedure could be developed to the extent that it would be extremely useful for obtaining more detailed information about individual cavitation craters.

e) The best single-property correlation between the material properties and cavitation volume loss for the mercury tests was obtained with the ultimate resilience, which appeared to the 1/2 power, just as was the case for all the vibratory cavitation damage data obtained by this laboratory, using water, mercury, lead-bismuth alloy, and lithium. However, no significant correlation was obtained between the water venturi damage data and ultimate resilience, perhaps because of the important and unknown role of corrosion in these tests.

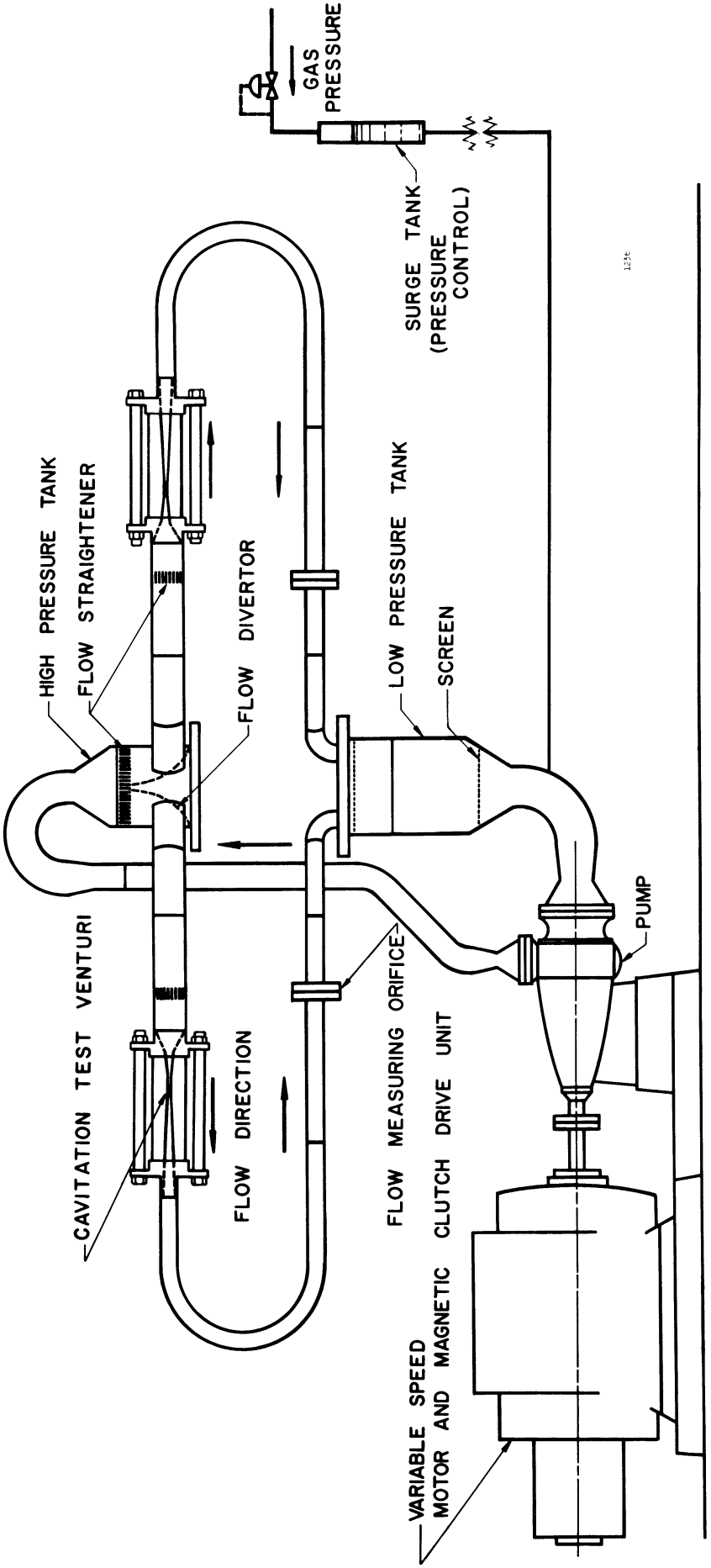

Fig. 1.--Schematic of water cavitation damage facility (only two of the four loops are shown).

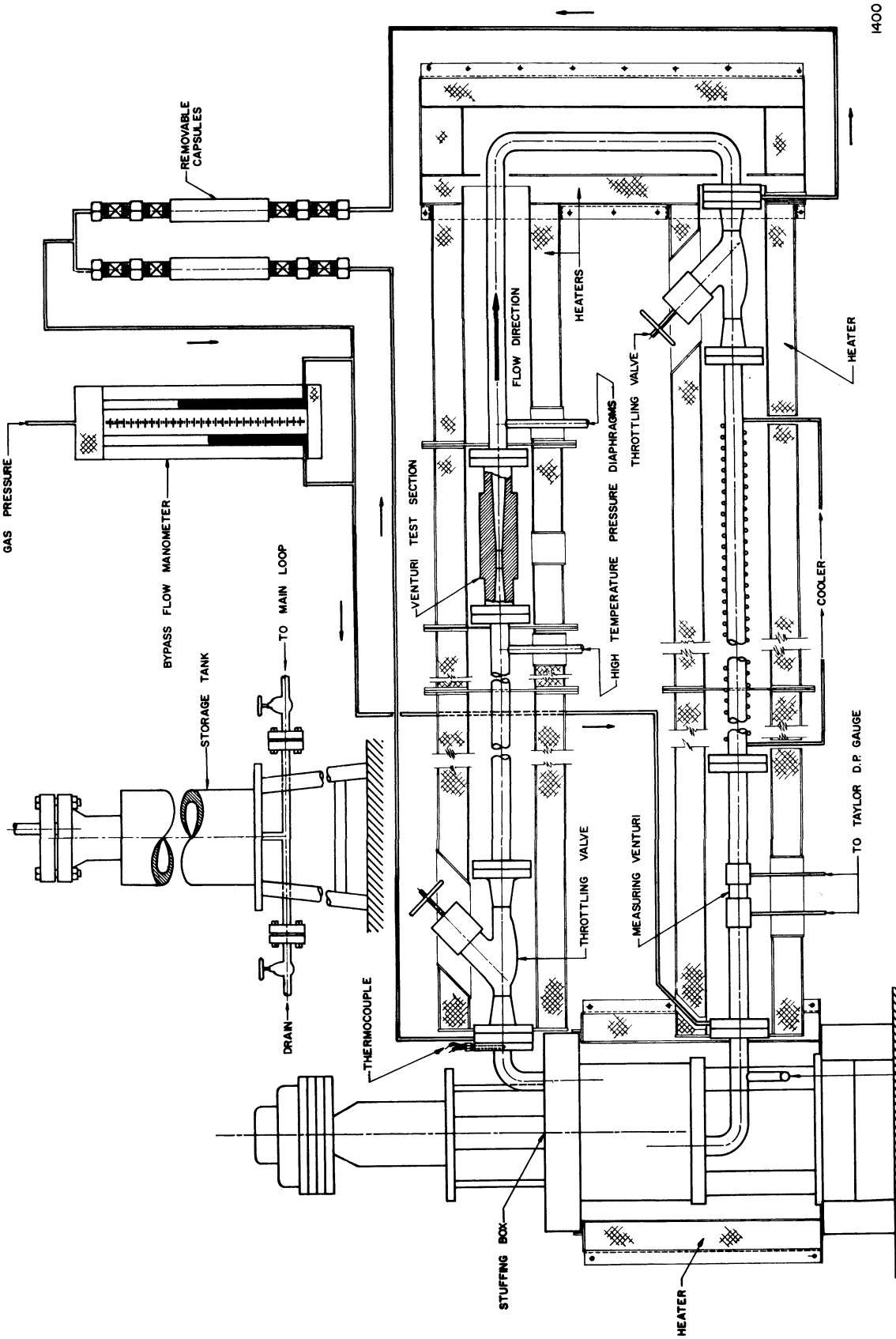

Fig. 2.--Schematic of mercury loop and sample bypass lines.

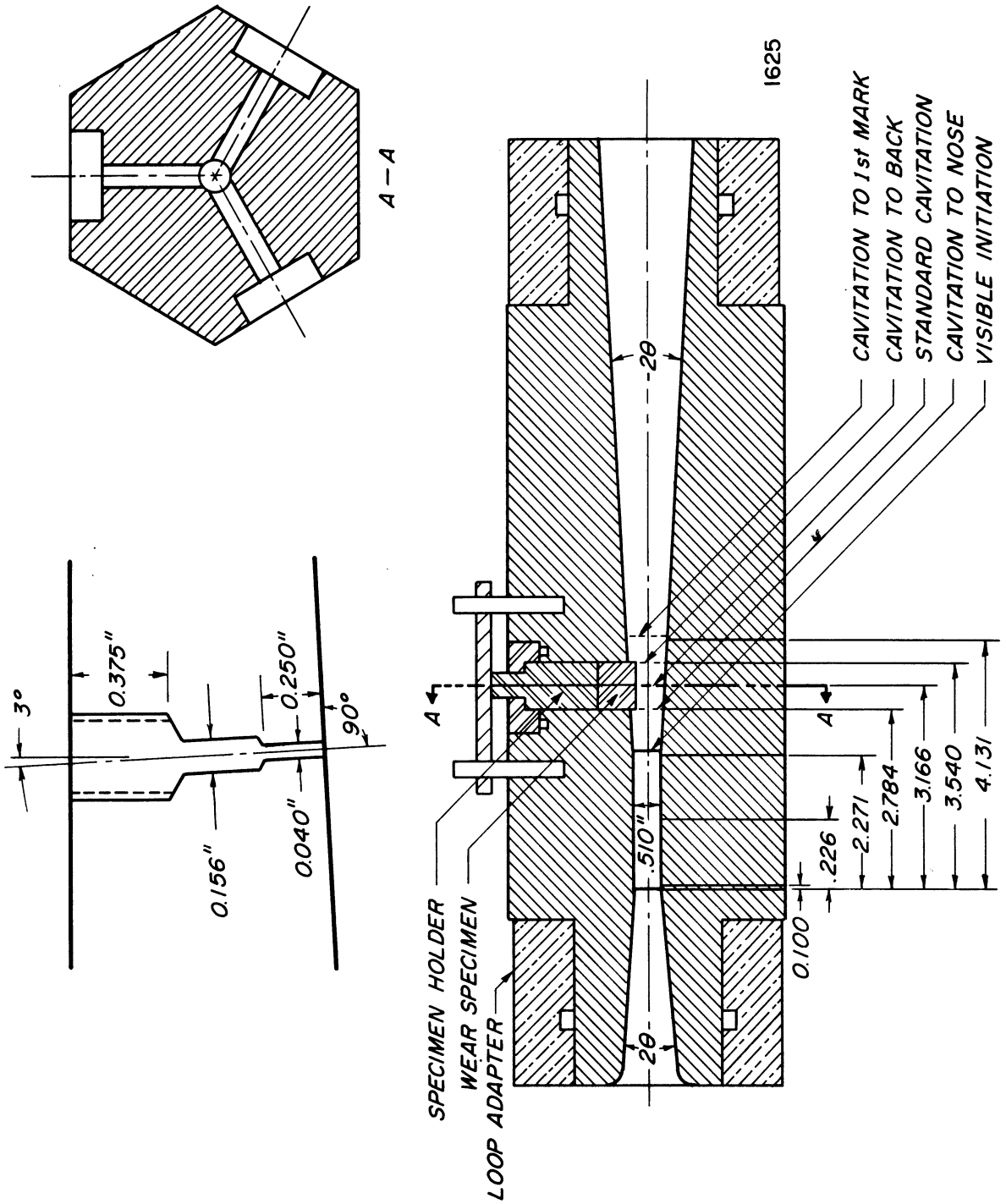

Fig. 3.--Cross section schematic drawing of damage venturi as modified for pressure profile measurements.

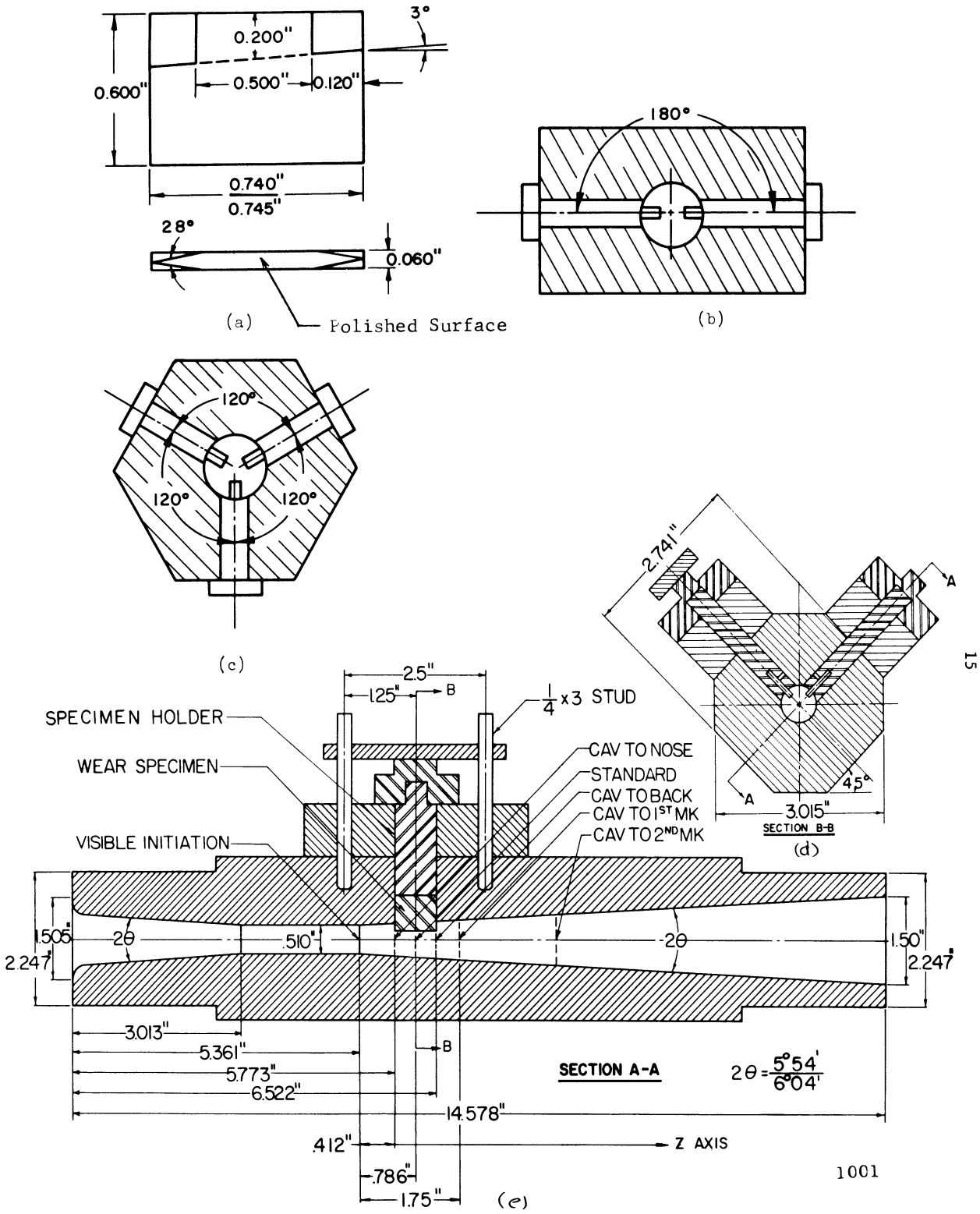

Fig. 4.--Schematic drawing of the damage test venturis showing nominal flow passage, axial specimen location, cavitation termination points, and (a) test specimen dimensions, (b) two specimen symmetrical arrangement for mercury, (c) three specimen symmetrical arrangement for water, (d) two specimen unsymmetrical arrangement for earlier mercury tests.

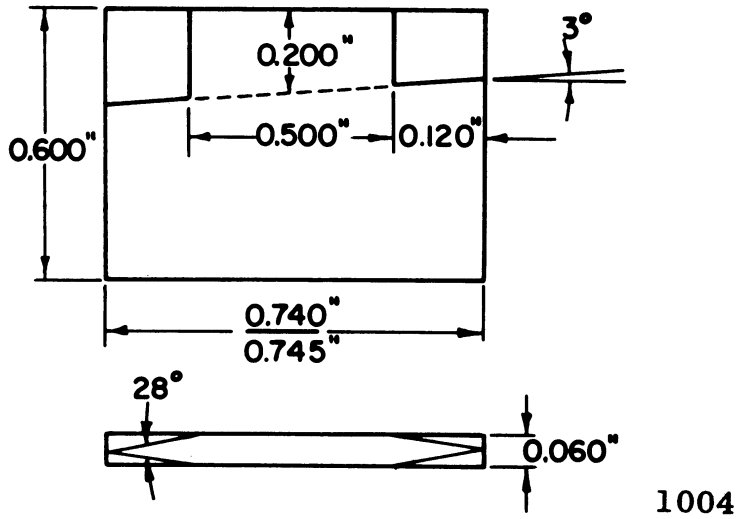

Drawing of Damage Specimen.

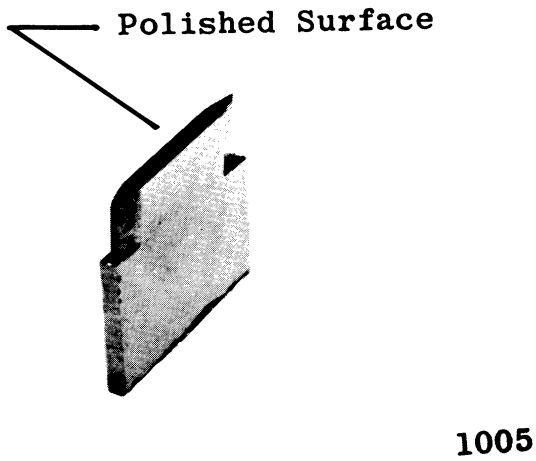

Fig. 5.--Drawing and photograph of damage specimen.

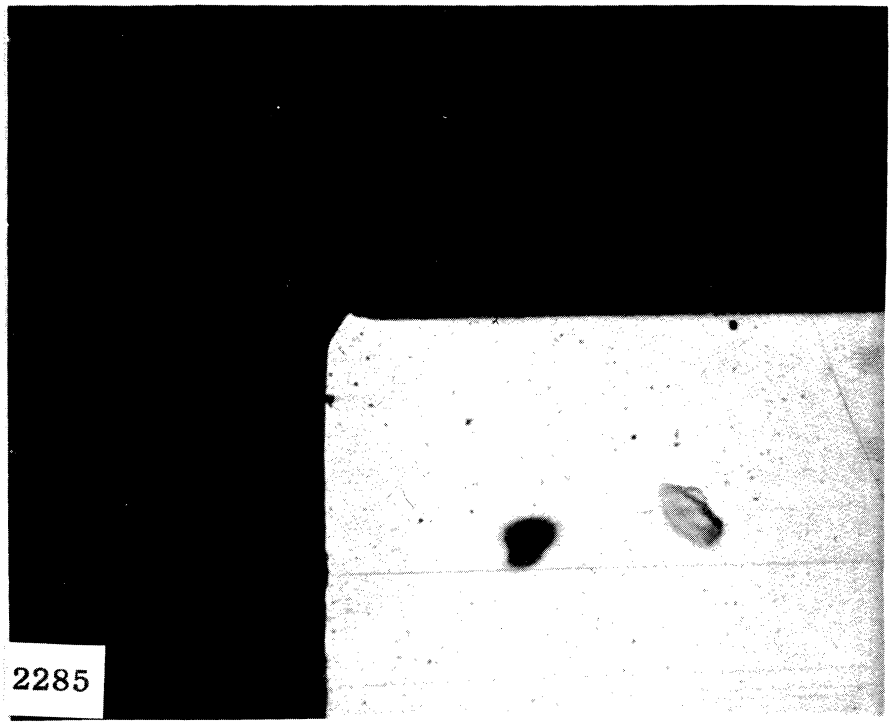

(a)

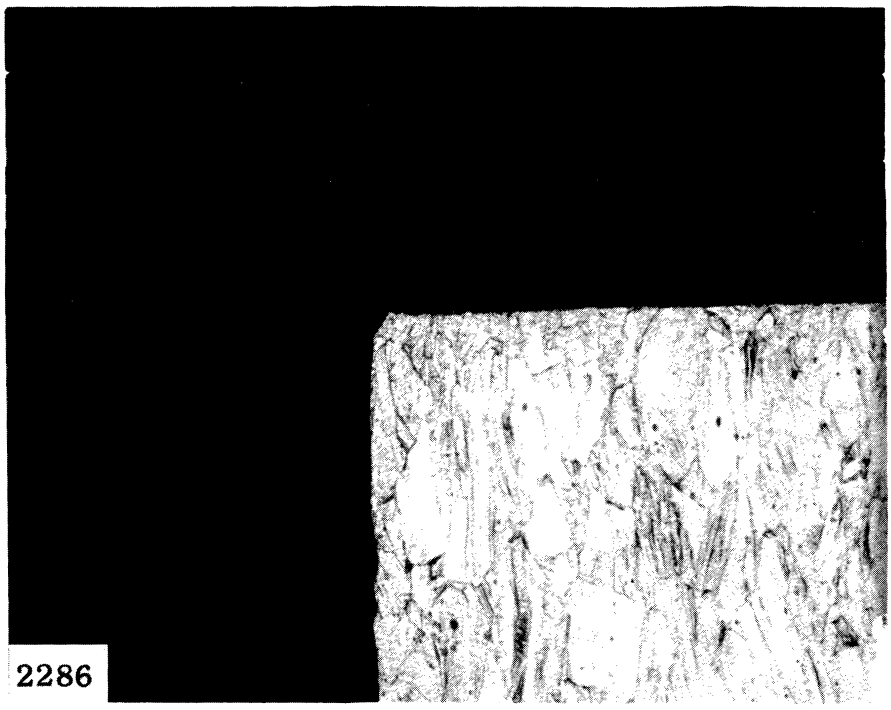

(b)

Fig. 6.--Photomicrographs of corner of specimen #CZ-7 (copper-zinc alloy, 60% cold-worked) after 100 hours exposure to "standard cavitation" in water (80°F) at a throat velocity of 200 feet per second. Magnification 250X. (a) Unetched, (b) Etched.

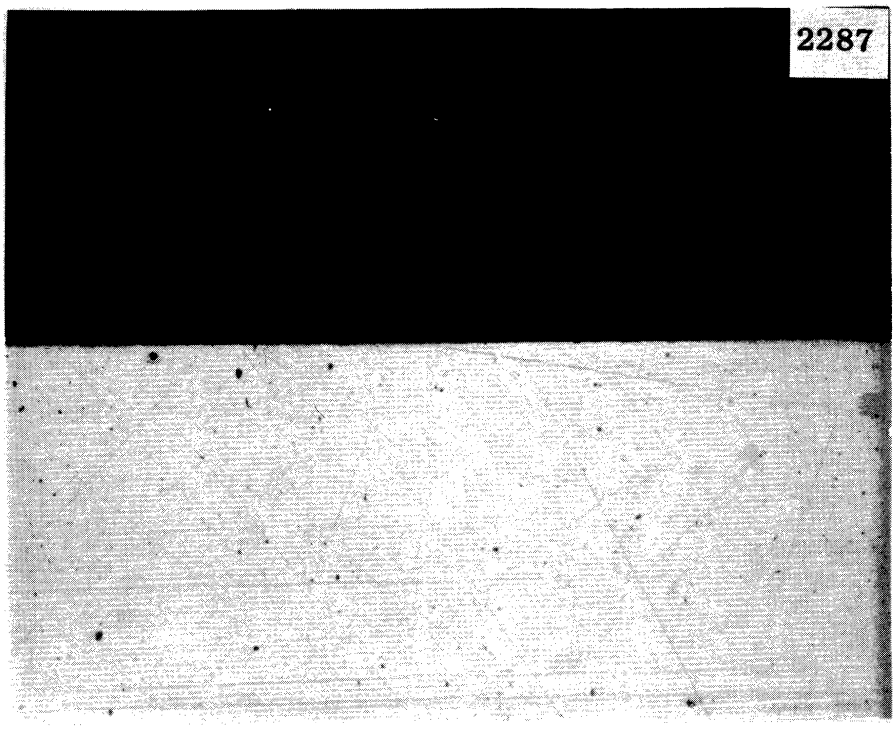

(a)

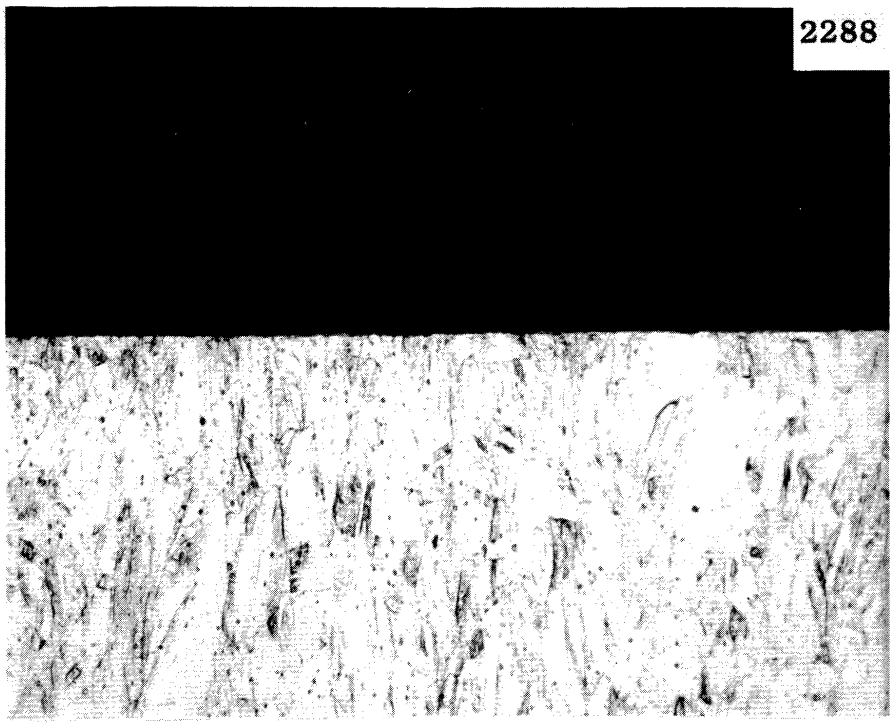

(b)

Fig. 7.--Photomicrographs of surface of specimen #CZ-7 (copper-zinc alloy, 60% cold-worked) after 100 hours exposure to "standard cavitation" in water (80°F) at a throat velocity of 200 feet per second. Magnification 250X. (a) Unetched, (b) Etched.

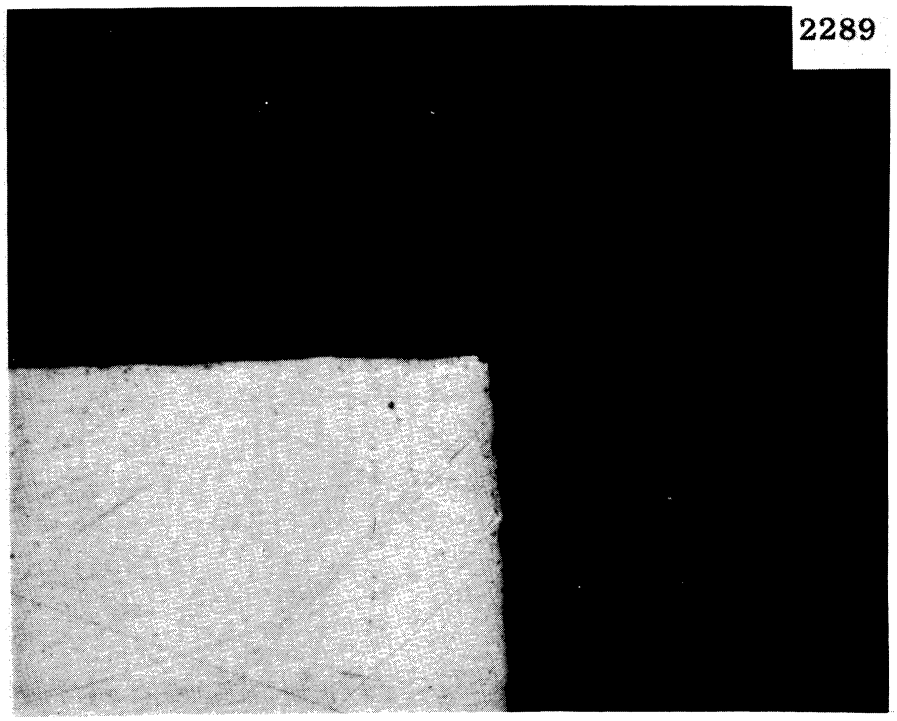

(a)

(b)

Fig. 8.--Photomicrographs of corner of specimen #CZ-79 (copper-zinc alloy, 850°F anneal, 1 hour) after 100 hours exposure to "standard cavitation" in water (80°F) at a throat velocity of 200 feet per second. Magnification 250X. (a) Unetched, (b) Etched.

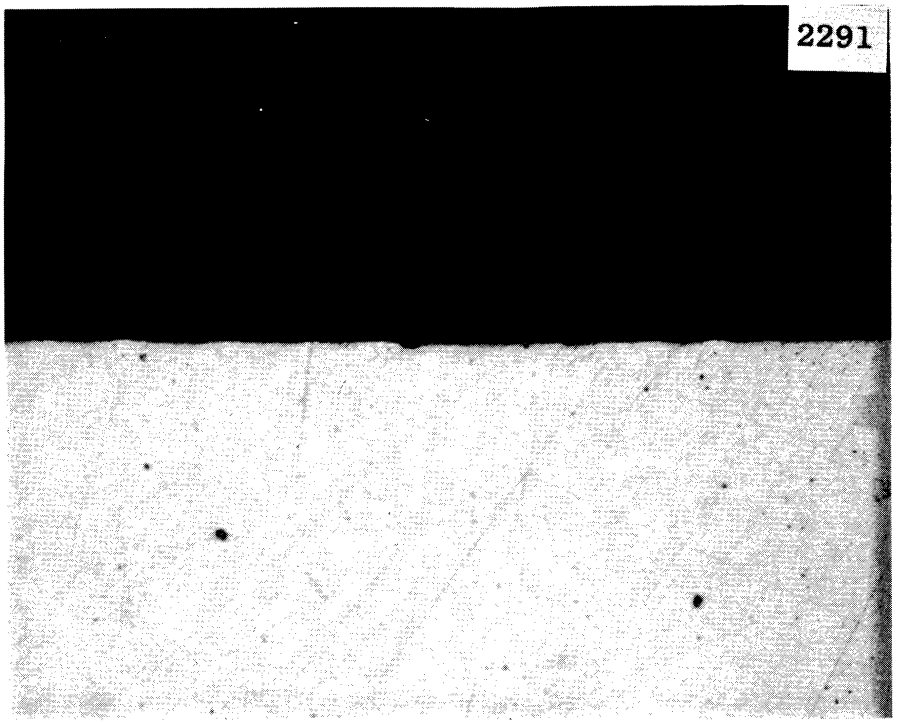

(a)

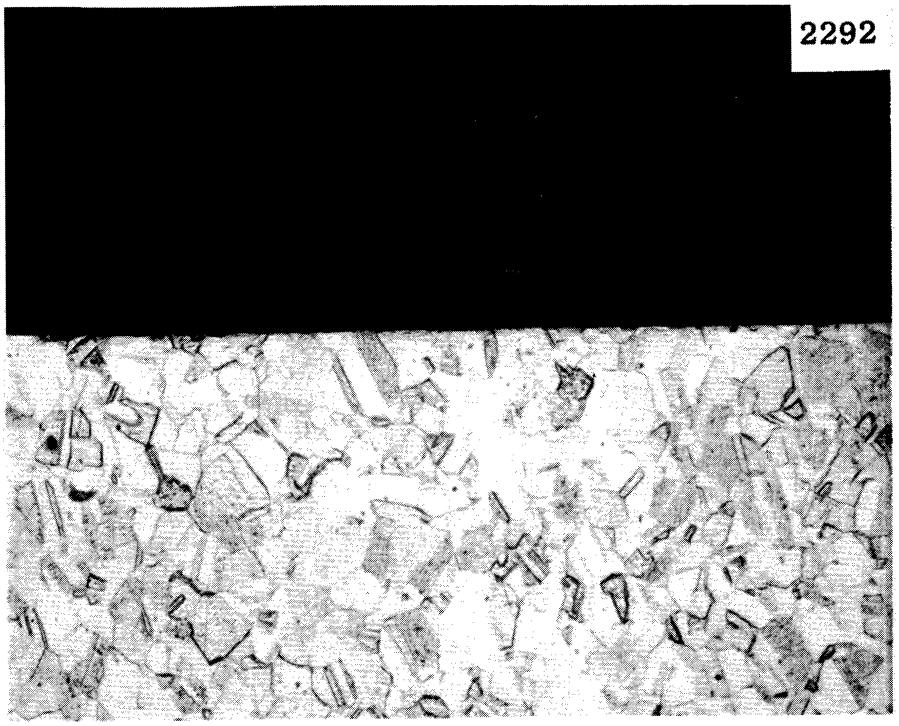

(b)

Fig. 9.--Photomicrographs of surface of specimen #CZ-79 (copper-zinc alloy, 850°F anneal, 1 hour) after 100 hours exposure to "standard cavitation" in water (80°F) at a throat velocity of 200 feet per second. Magnification 250X. (a) Unetched, (b) Etched.

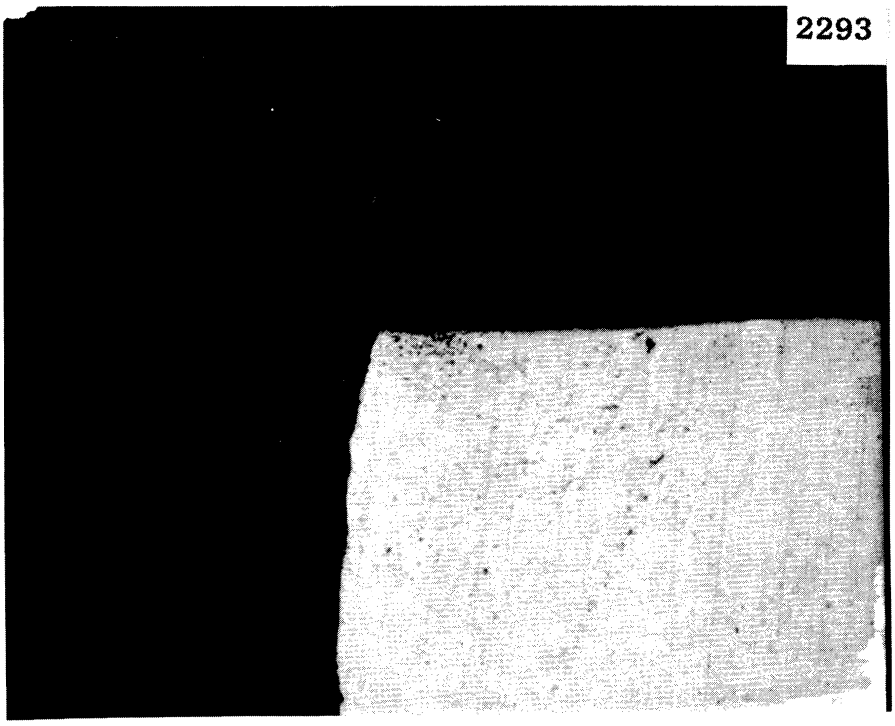

(a)

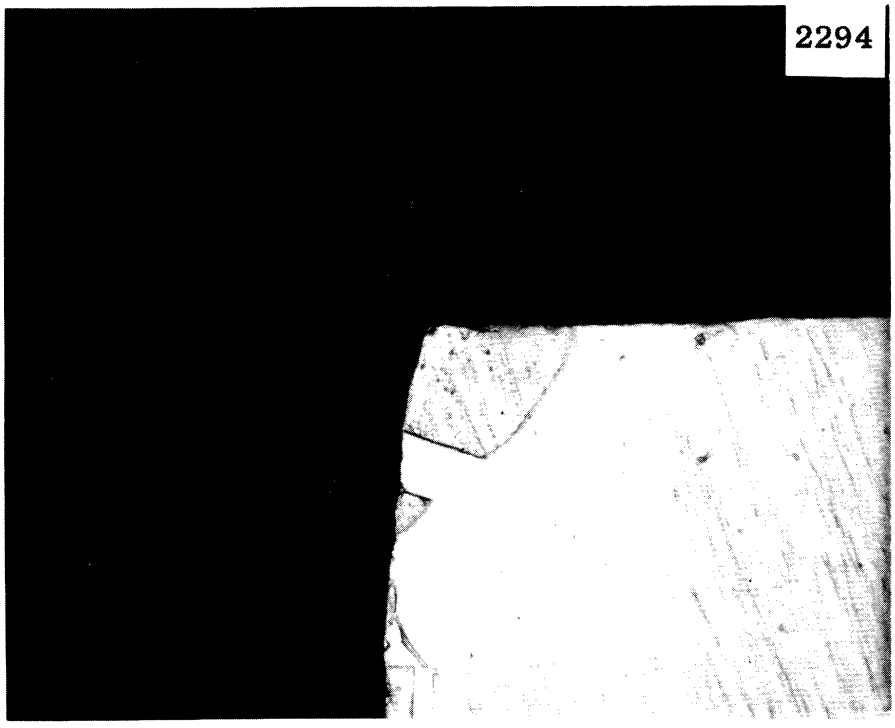

(b)

Fig. 10.--Photomicrographs of corner of specimen #CZ-229 (copper-zinc alloy, 1400°F anneal, 1 hour) after 100 hours exposure to "standard cavitation" in water (80°F) at a throat velocity of 200 feet per second. Magnification 250X. (a) Unetched, (b) Etched.

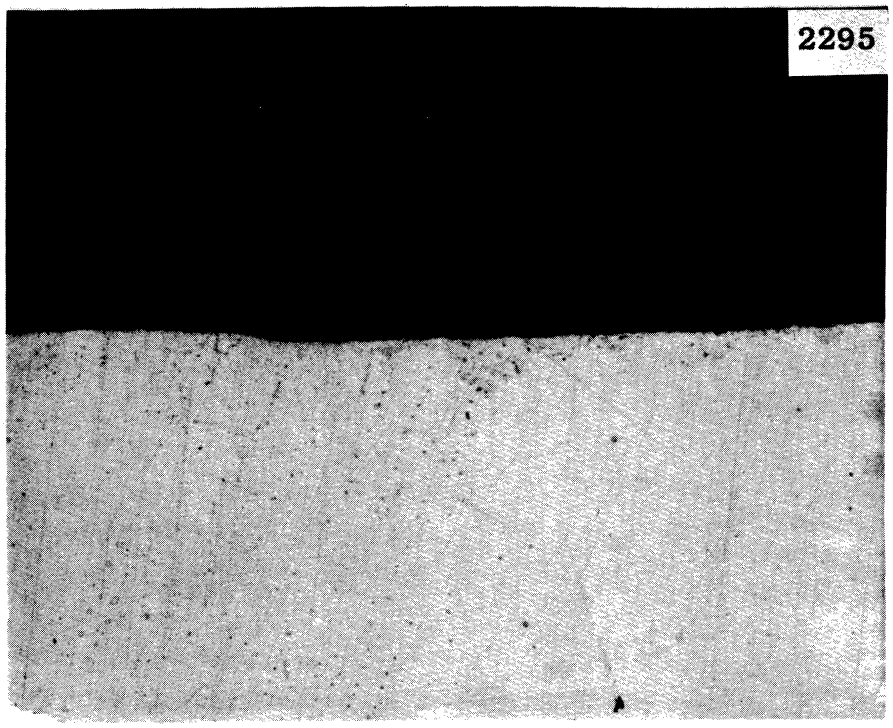

(a)

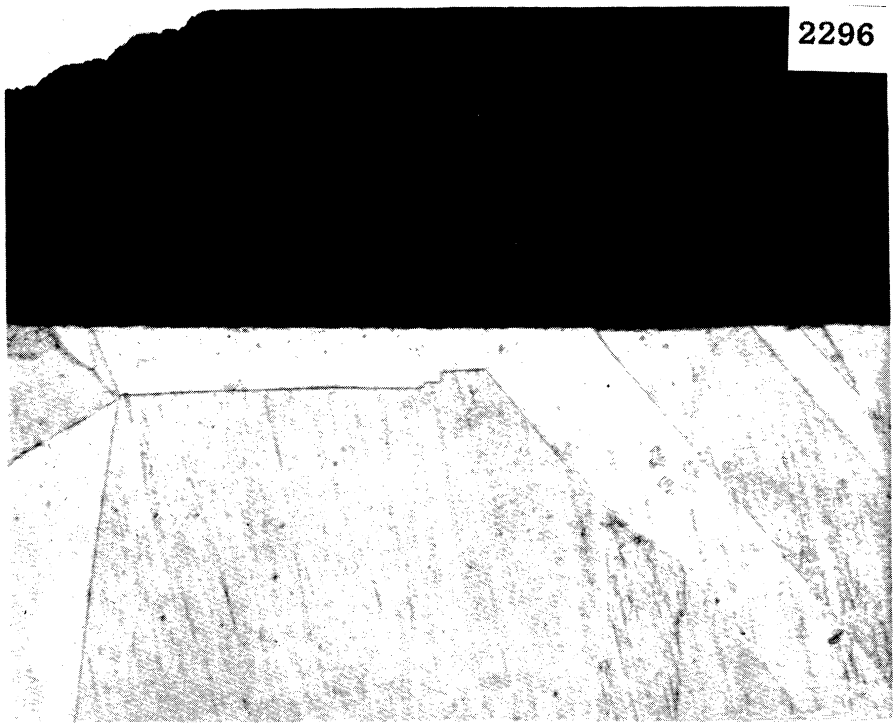

(b)

Fig. 11.--Photomicrographs of surface of specimen #CZ-229 (copper-zinc alloy, 1400°F anneal, 1 hour) after 100 hours exposure to "standard cavitation" in water (80°F) at a throat velocity of 200 feet per second. Magnification 250X. (a) Unetched, (b) Etched.

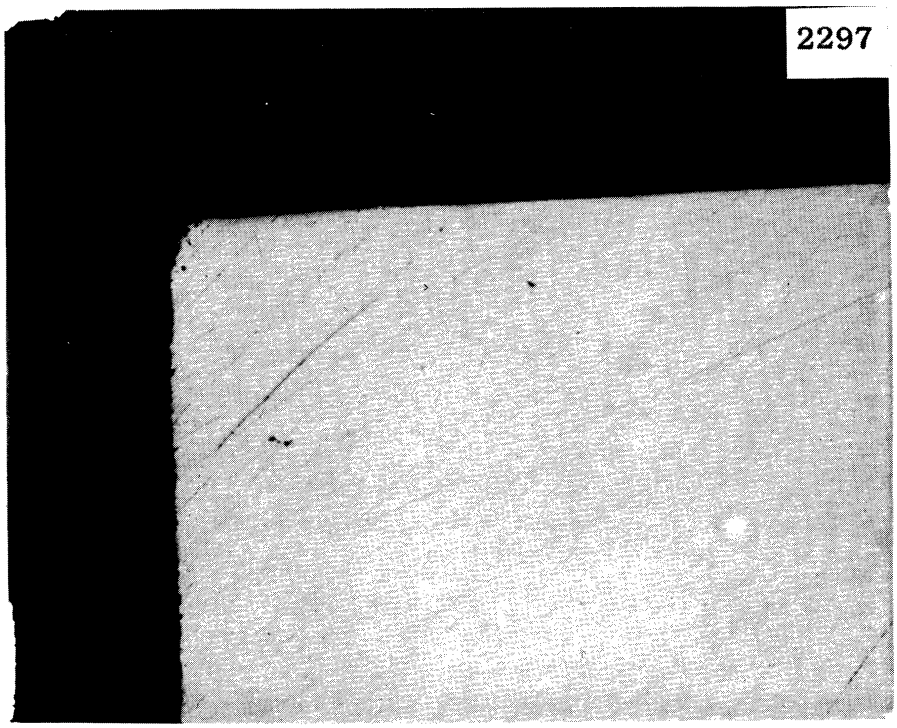

(a)

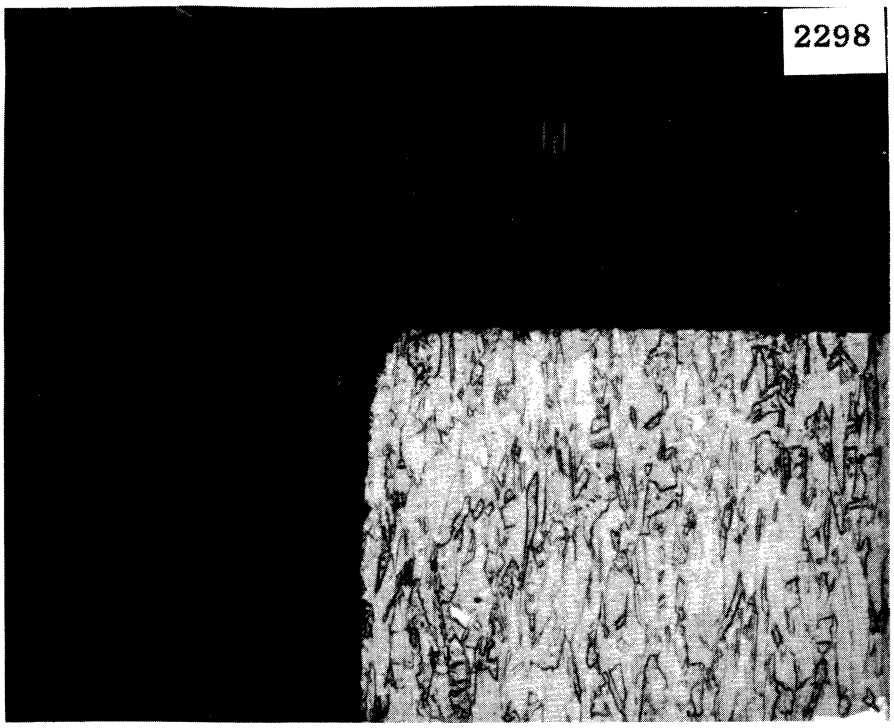

(b)

Fig. 12.--Photomicrographs of corner of specimen #Cu-7 (copper, 60% cold-worked) after 100 hours exposure to "standard cavitation" in water (80°F) at a throat velocity of 200 feet per second. Magnification 250X. (a) Unetched, (b) Etched.

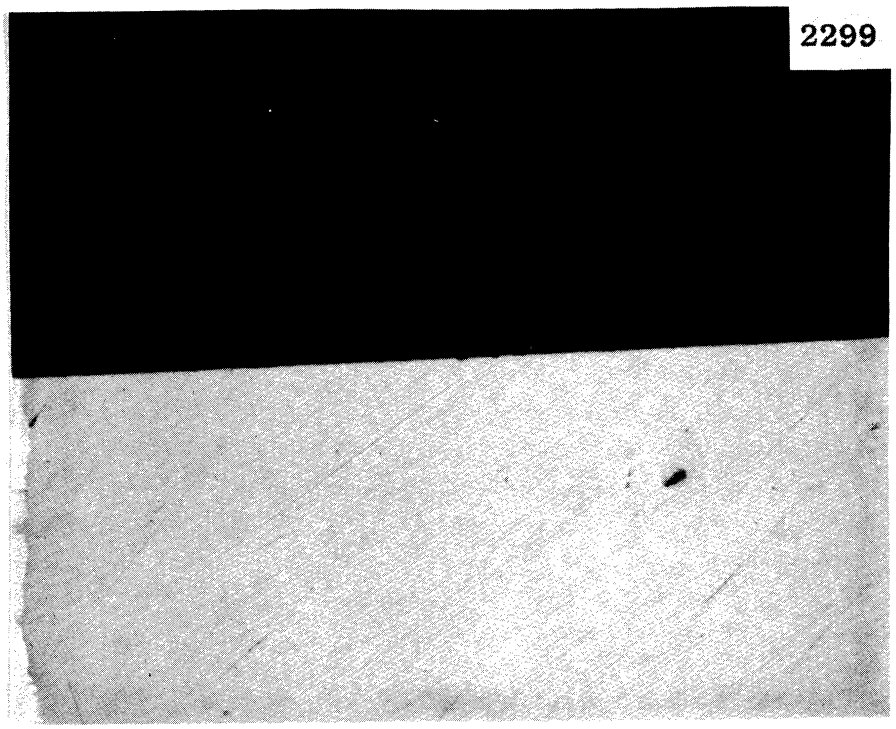

(a)

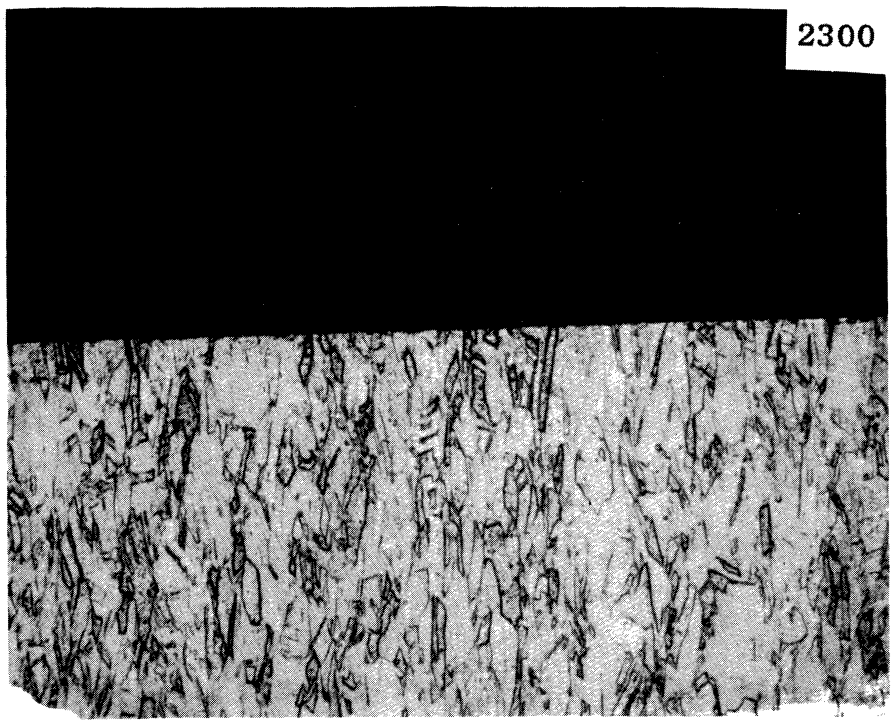

(b)

Fig. 13.--Photomicrographs of surface of specimen #Cu-7 (copper, 60% cold-worked) after 100 hours exposure to "standard cavitation" in water (80°F) at a throat velocity of 200 feet per second. Magnification 250X. (a) Unetched, (b) Etched.

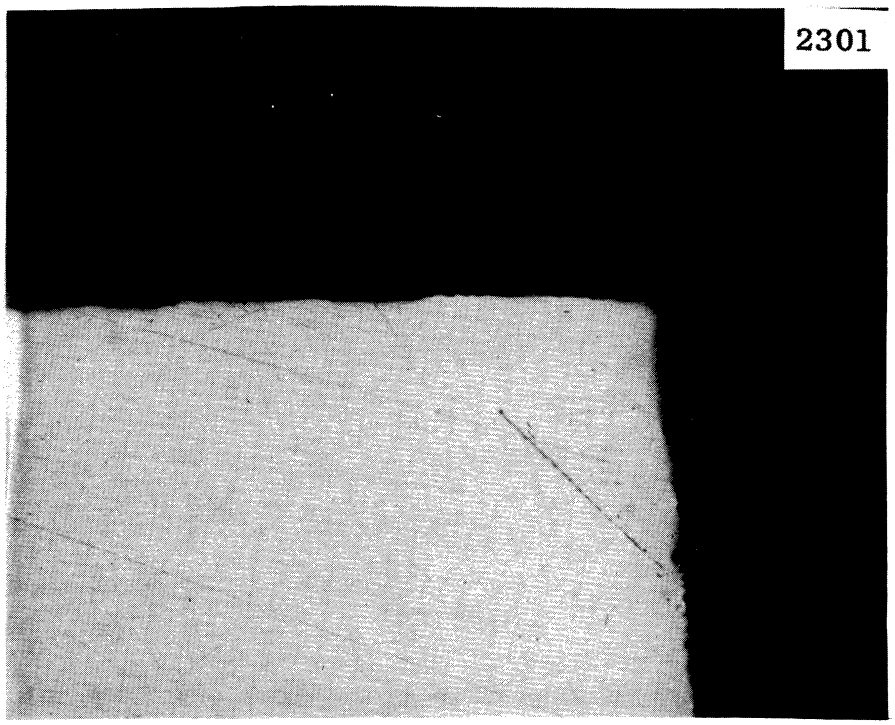

(a)

(b)

Fig. 14.--Photomicrographs of corner of specimen #Cu-83 (copper, 900°F anneal, 1 hour) after 100 hours exposure to "standard cavitation" in water (80°F) at a throat velocity of 200 feet per second. Magnification 250X. (a) Unetched, (b) Etched.

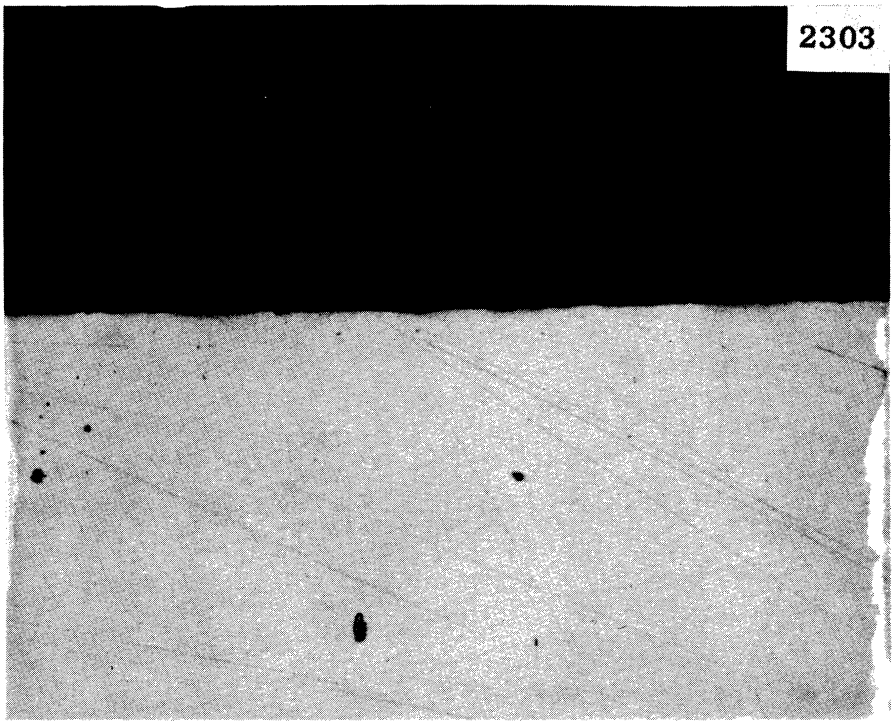

(a)

(b)

Fig. 15.--Photomicrographs of surface of specimen #Cu-83 (copper, 900°F anneal, 1 hour) after 100 hours exposure to "standard cavitation" in water (80°F) at a throat velocity of 200 feet per second. Magnification 250X. (a) Unetched, (b) Etched.

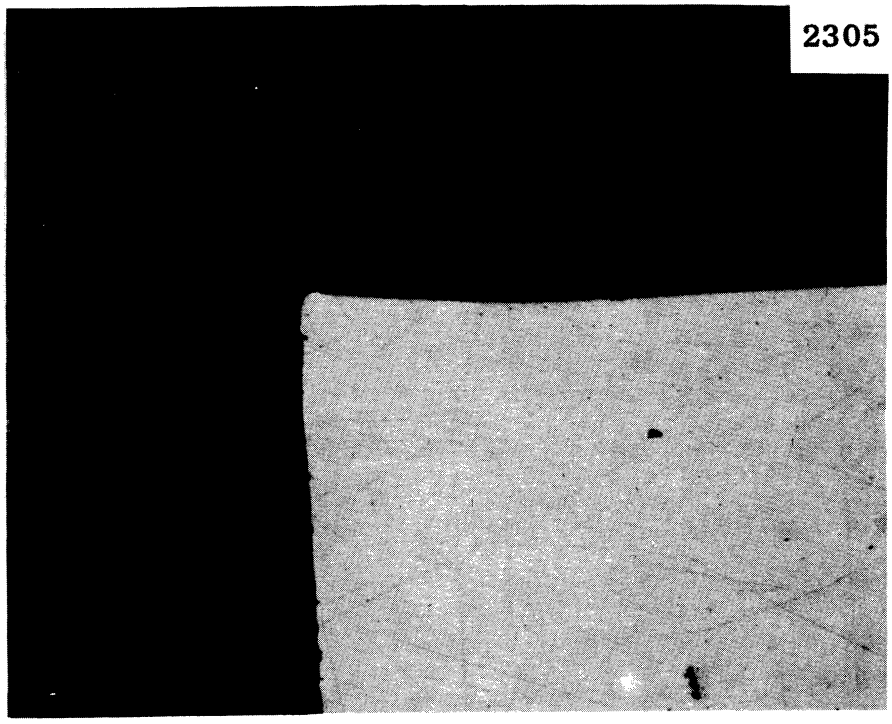

(a)

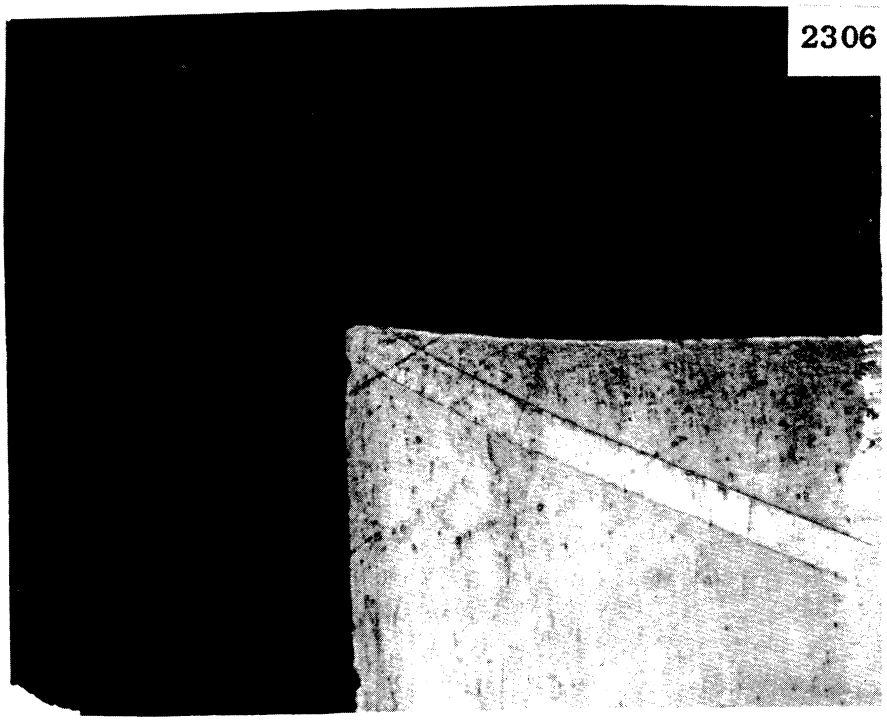

(b)

Fig. 16.--Photomicrographs of corner of specimen #Cu-157 (copper, 1500°F anneal, 1 hour) after 100 hours exposure to "standard cavitation" in water (80°F) at a throat velocity of 200 feet per second. Magnification 250X. (a) Unetched, (b) Etched.

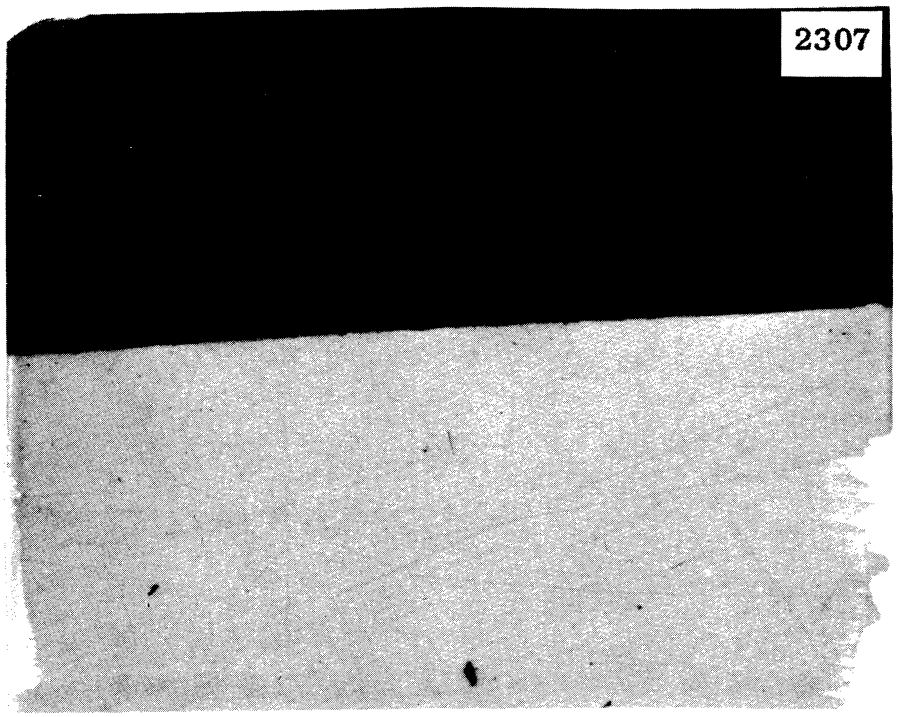

(a)

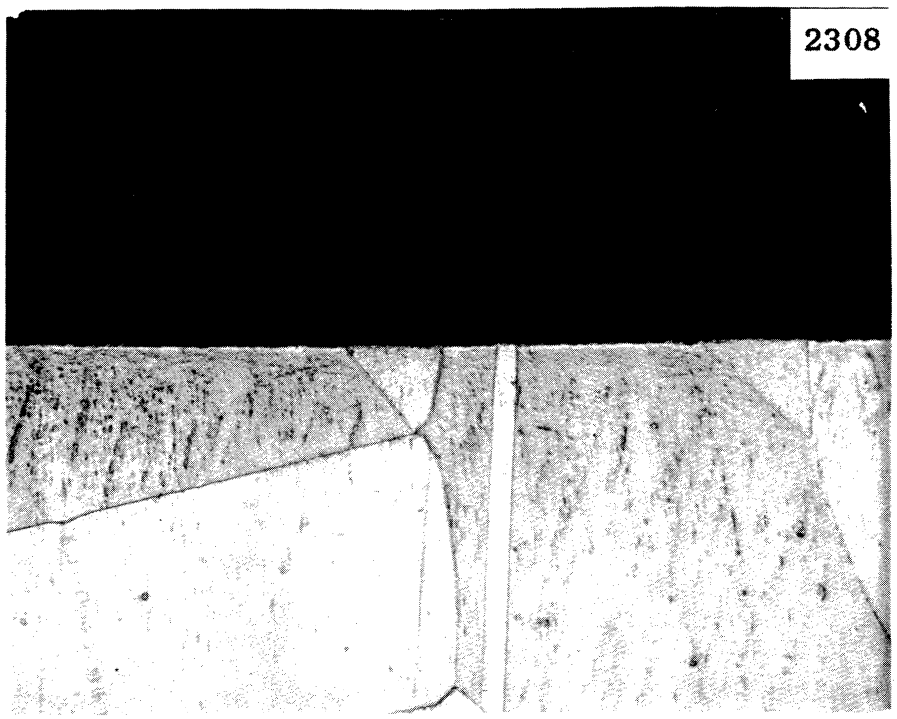

(b)

Fig. 17.--Photomicrographs of surface of specimen #Cu-157 (copper, 1500°F anneal, 1 hour) after 100 hours exposure to "standard cavitation" in water (80°F) at a throat velocity of 200 feet per second. Magnification 250X. (a) Unetched, (b) Etched.

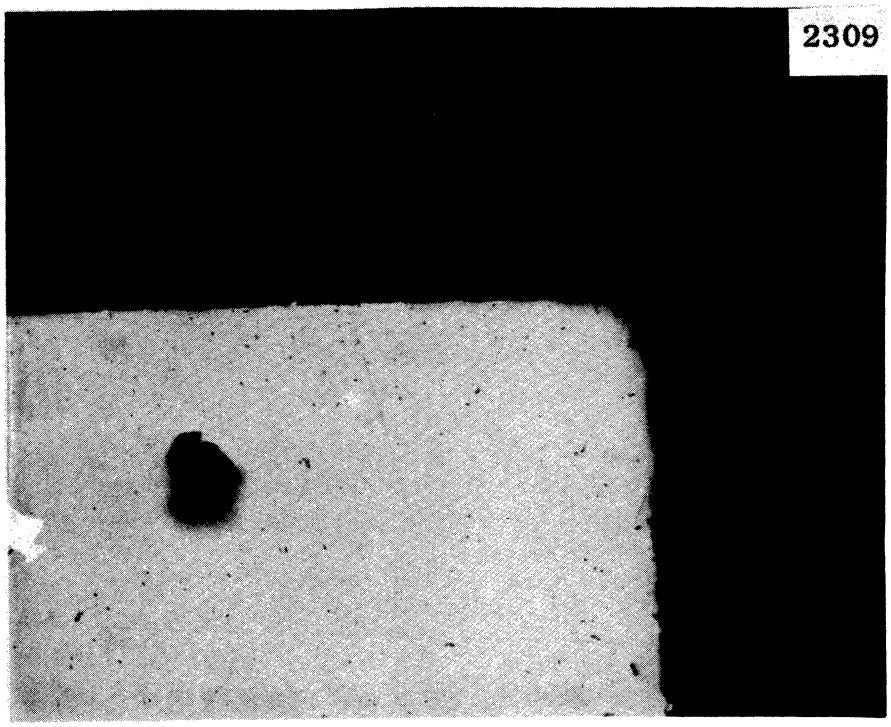

(a)

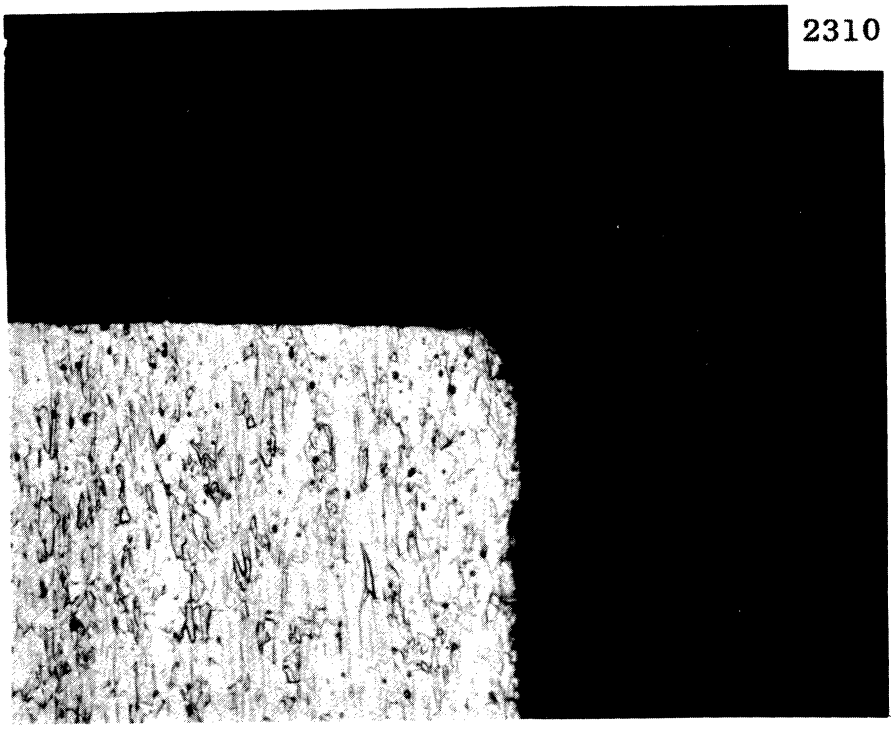

(b)

Fig. 18.--Photomicrographs of corner of specimen #Cu-Ni-10 (copper-nickel alloy, 60% cold-worked) after 100 hours exposure to "standard cavitation" in water (80°F) at a throat velocity of 200 feet per second. Magnification 250X. (a) Unetched, (b) Etched.

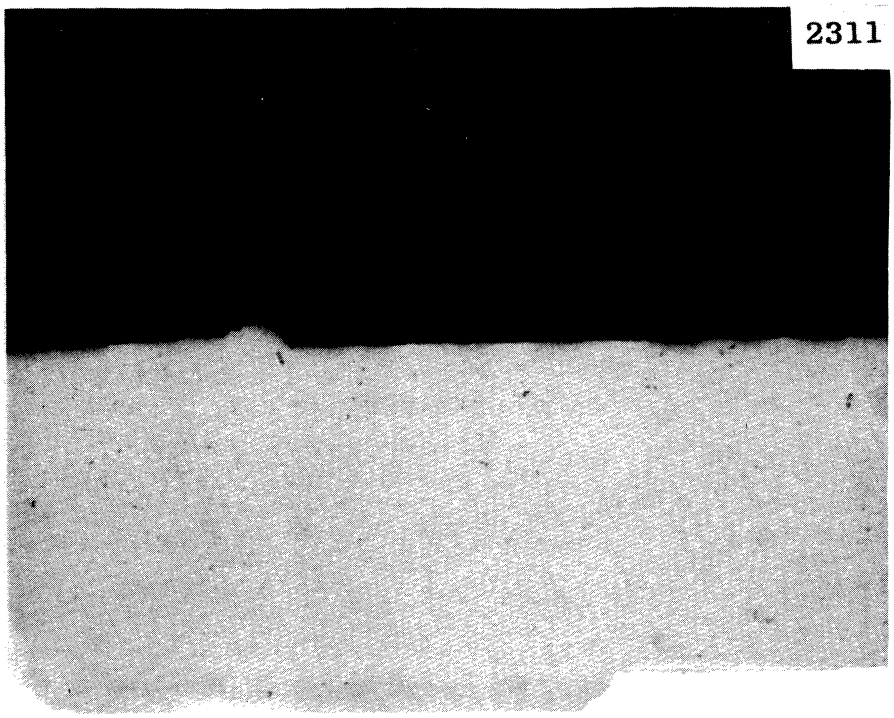

(a)

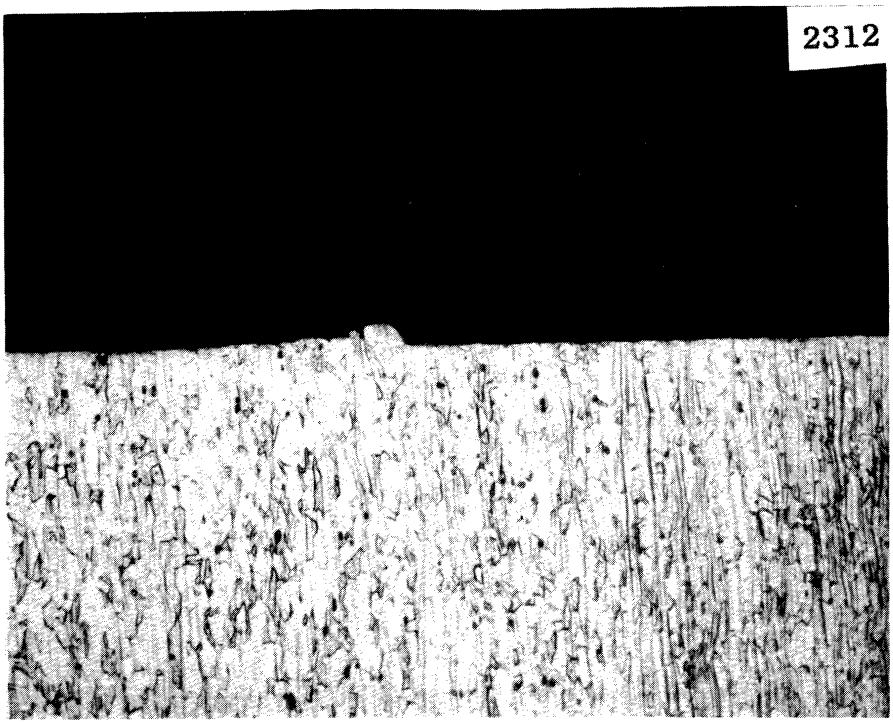

(b)

Fig. 19.--Photomicrographs of surface of specimen #Cu-Ni-10 (copper-nickel alloy, 60% cold-worked) after 100 hours exposure to "standard cavitation" in water (80°F) at a throat velocity of 200 feet per second. Magnification 250X. (a) Unetched, (b) Etched.

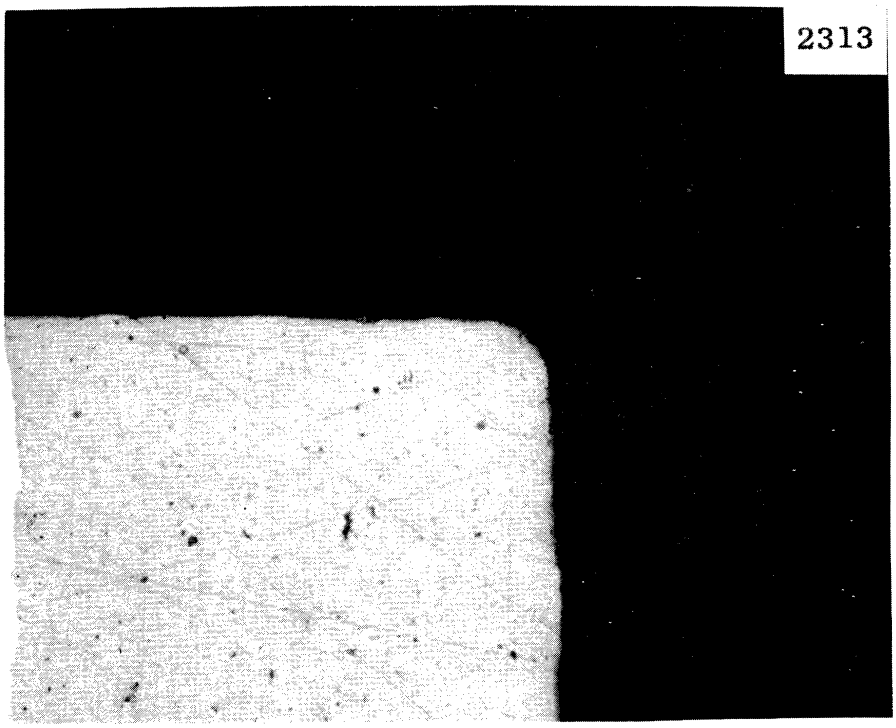

(a)

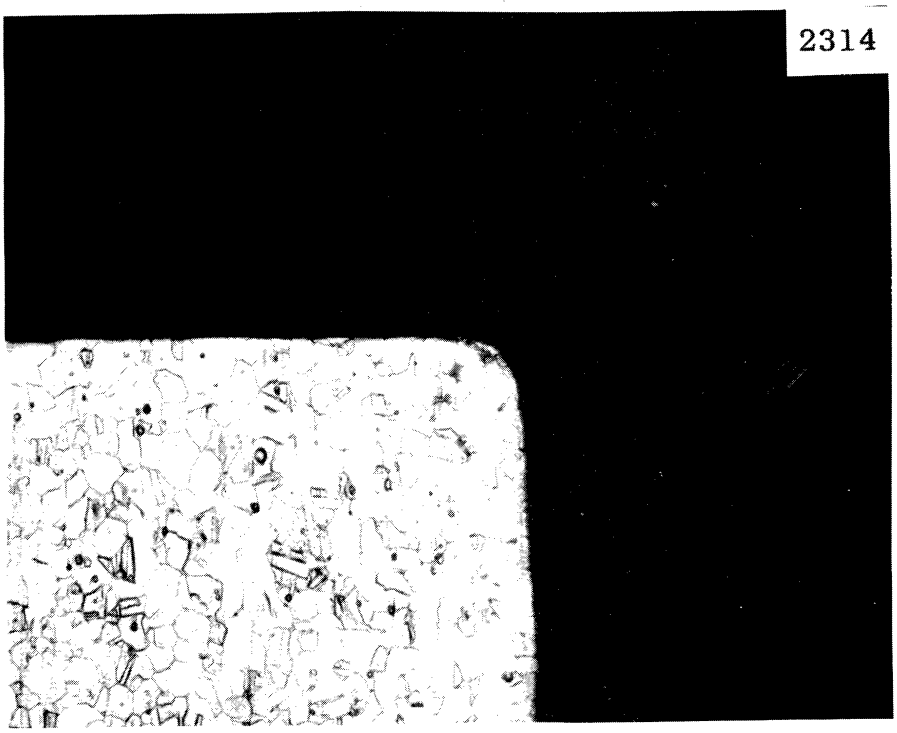

(b)

Fig. 20.--Photomicrographs of corner of specimen #Cu-Ni-84 (copper-nickel alloy, 1300°F anneal, 1 hour) after 100 hours exposure to "standard cavitation" in water (80°F) at a throat velocity of 200 feet per second. Magnification 250X. (a) Unetched, (b) Etched.

(a)

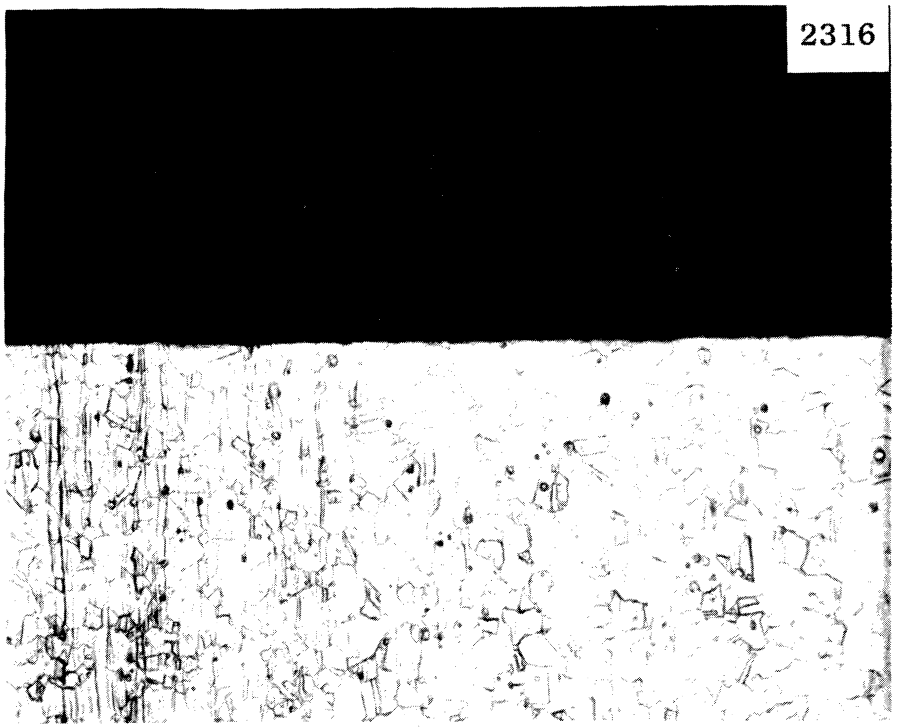

(b)

Fig. 21.--Photomicrographs of surface of specimen #Cu-Ni-84 (copper-nickel alloy, 1300°F anneal, 1 hour) after 100 hours exposure to "standard cavitation" in water (80°F) at a throat velocity of 200 feet per second. Magnification 250X. (a) Unetched, (b) Etched.

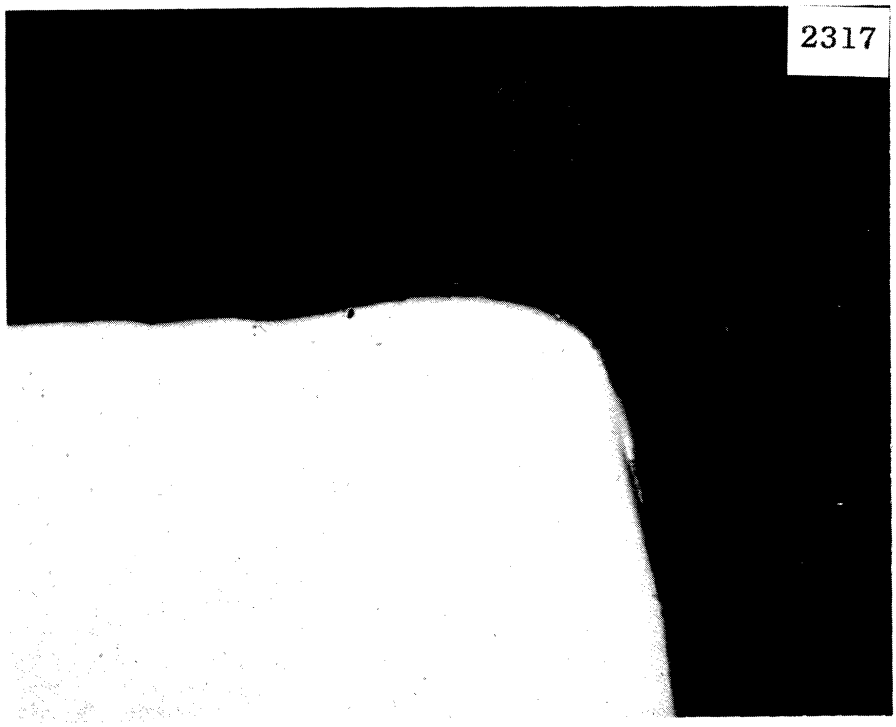

Fig. 22.--Photomicrograph of corner of specimen #Cu-Ni-153 (copper-nickel alloy, 1800°F anneal, 1 hour) after 100 hours exposure to "standard cavitation" in water (80°F) at a throat velocity of 200 feet per second. Magnification 250X. Unetched specimen.

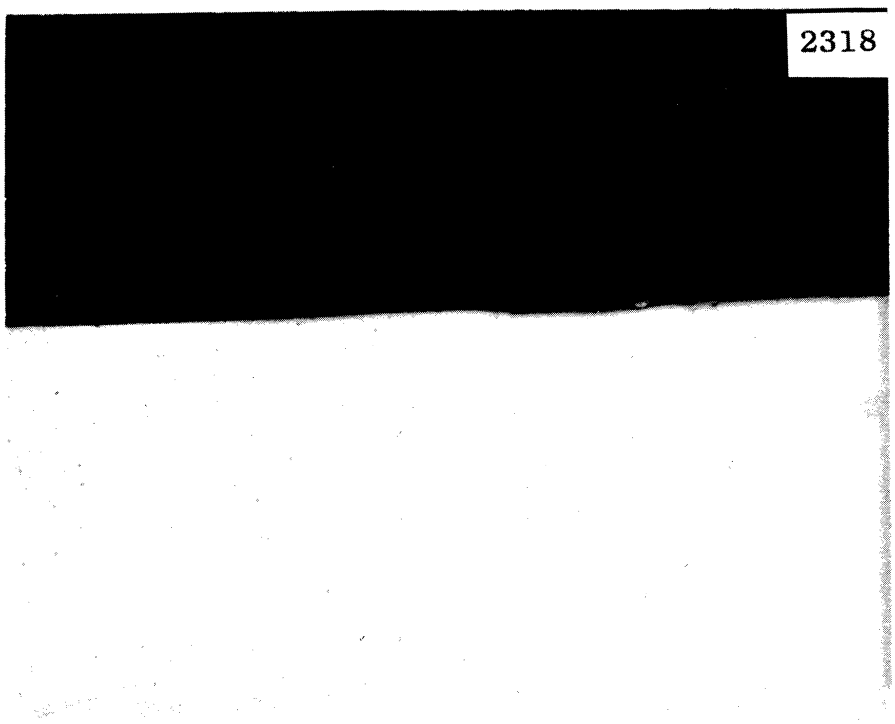

Fig. 23.--Photomicrograph of surface of specimen #Cu-Ni-153 (copper-nickel alloy, 1800°F anneal, 1 hour) after 100 hours exposure to "standard cavitation" in water (80°F) at a throat velocity of 200 feet per second. Magnification 250X. Unetched specimen.

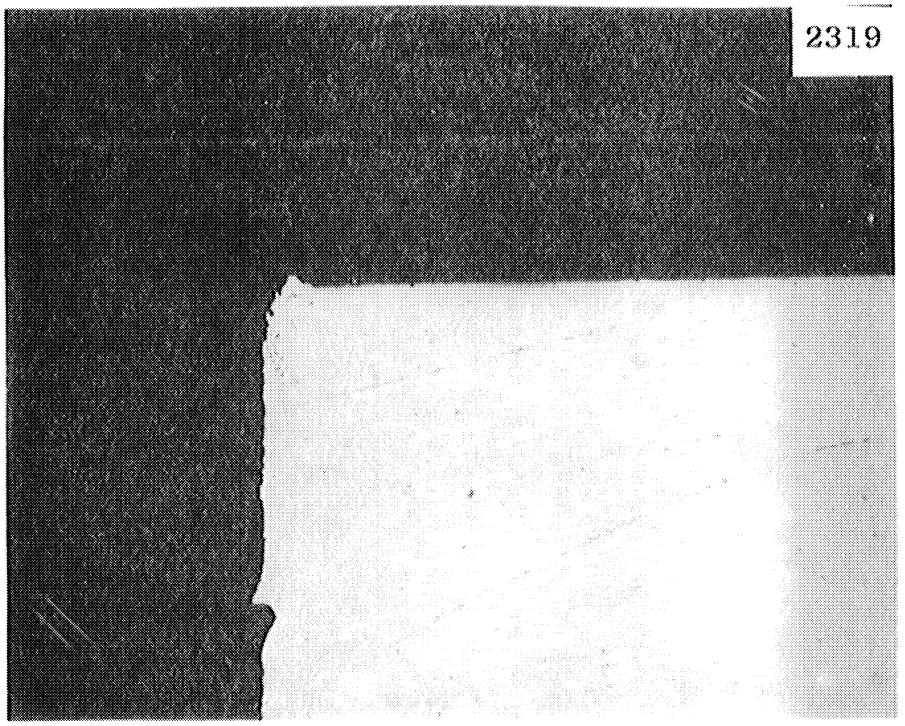

(a)

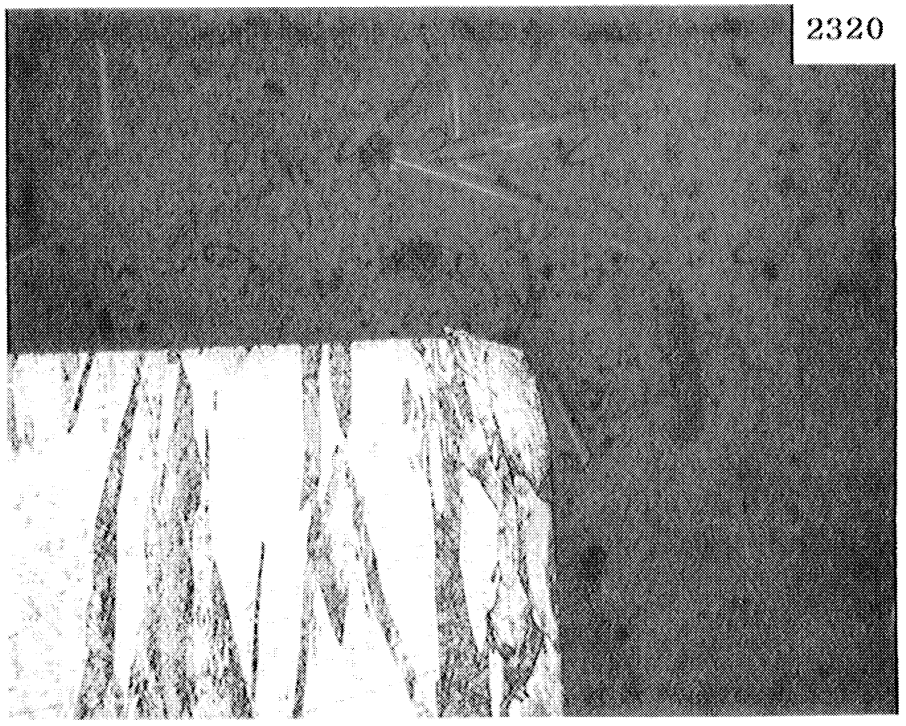

(b)

Fig. 24.--Photomicrographs of corner of specimen #Ni-11 (nickel, 75% cold-worked) after 100 hours exposure to "standard cavitation" in water (80°F) at a throat velocity of 200 feet per second. Magnification 250X. (a) Unetched, (b) Etched.

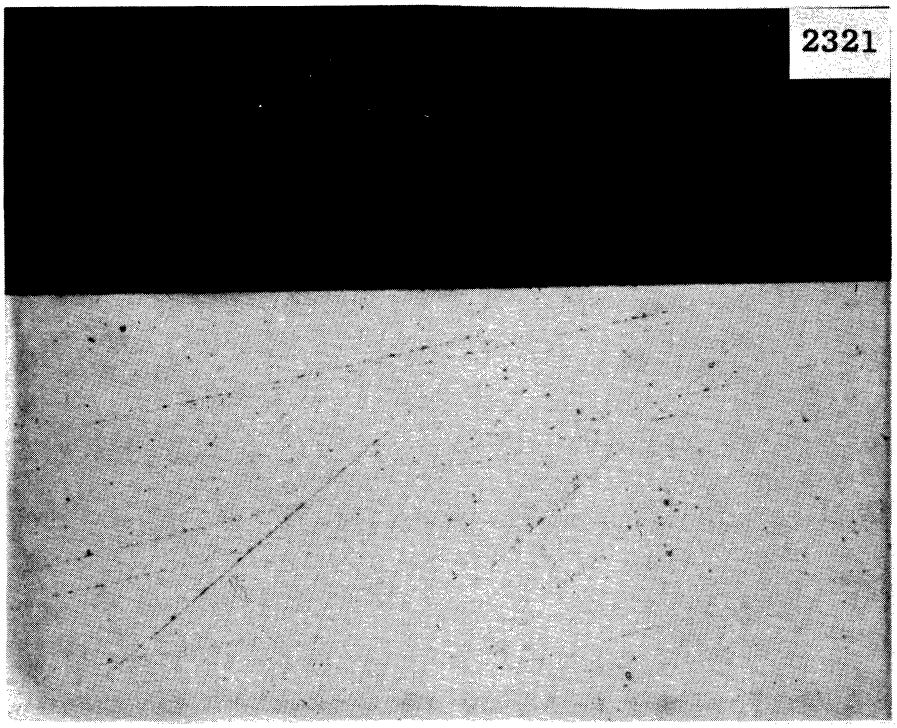

(a)

(b)

Fig. 25.--Photomicrographs of surface of specimen #Ni-11 (nickel, 75% cold-worked) after 100 hours exposure to "standard cavitation" in water (80°F) at a throat velocity of 200 feet per second. Magnification 250X. (a) Unetched, (b) Etched.

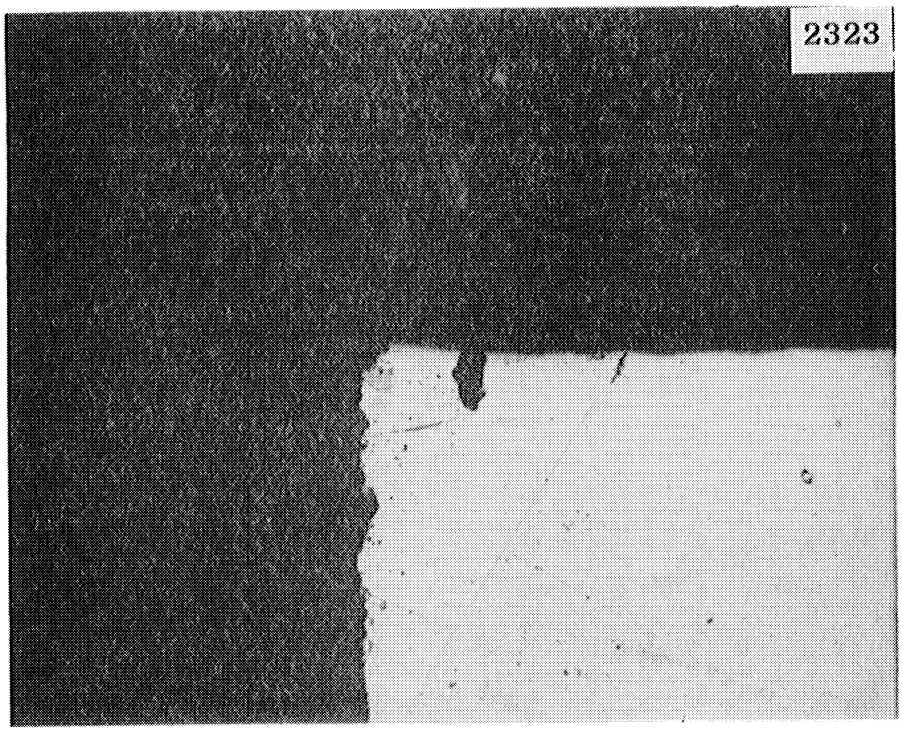

(a)

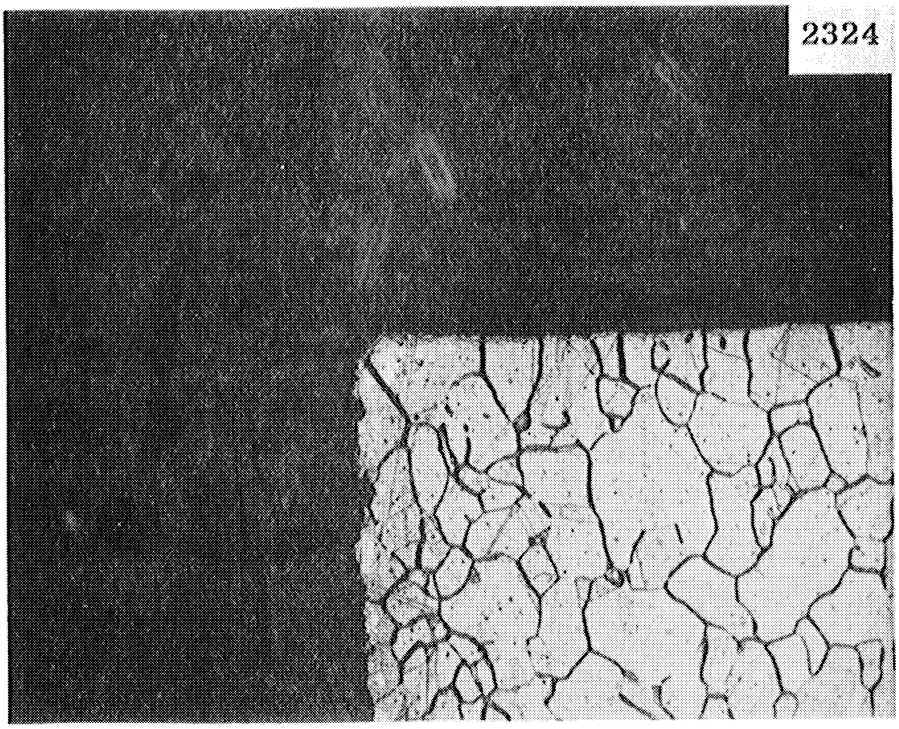

(b)

Fig. 26.--Photomicrographs of corner of specimen #Ni-83 (nickel, 1100°F anneal, 1 hour) after 100 hours exposure to "standard cavitation" in water (80°F) at a throat velocity of 200 feet per second. Magnification 250X. (a) Unetched, (b) Etched.

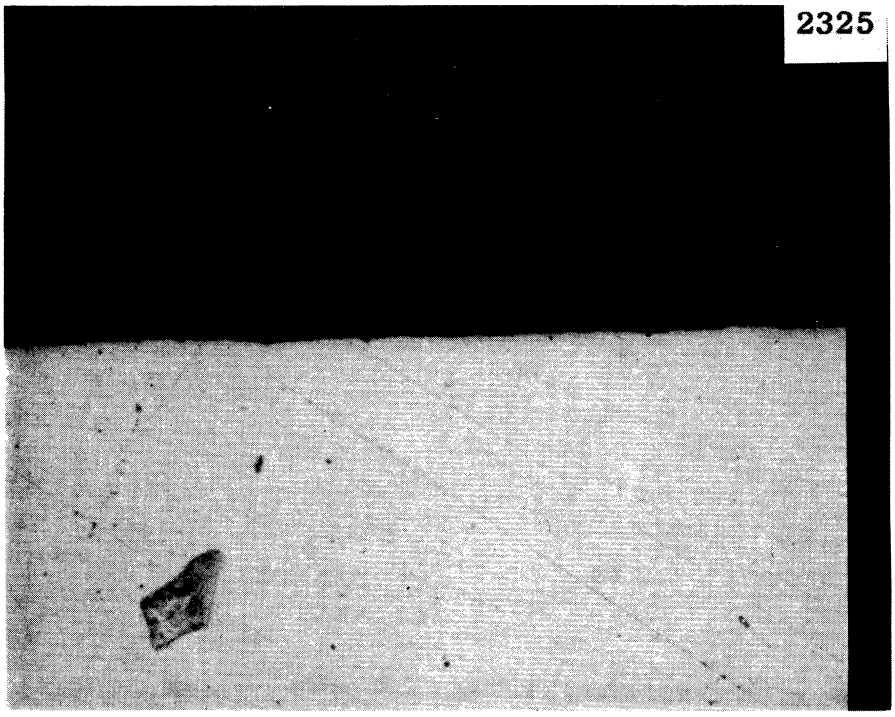

(a)

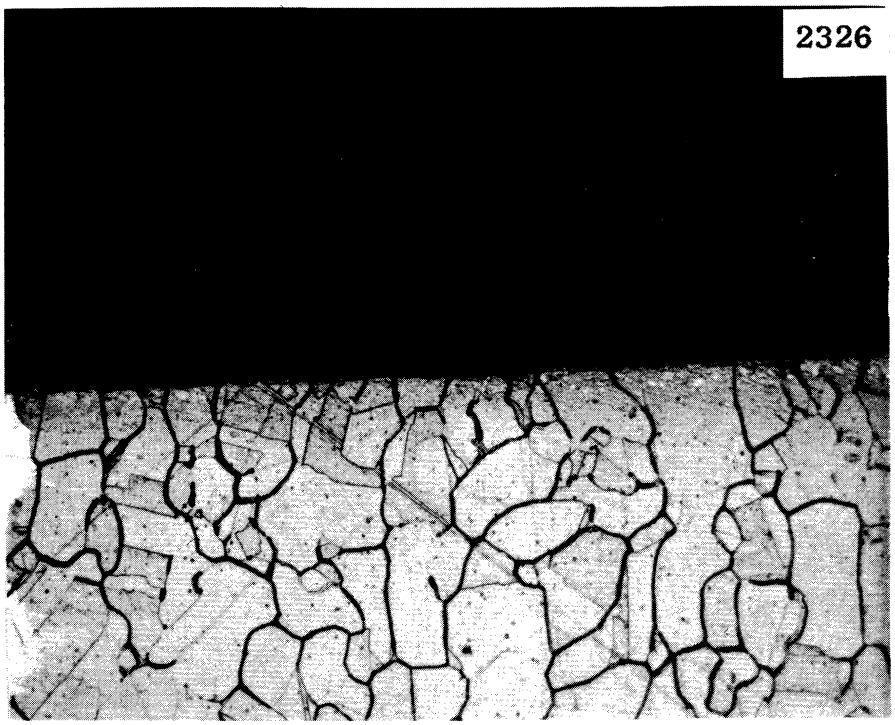

(b)

Fig. 27.--Photomicrographs of surface of specimen #Ni-83 (nickel, 1100°F anneal, 1 hour) after 100 hours exposure to "standard cavitation" in water (80°F) at a throat velocity of 200 feet per second. Magnification 250X. (a) Unetched, (b) Etched.

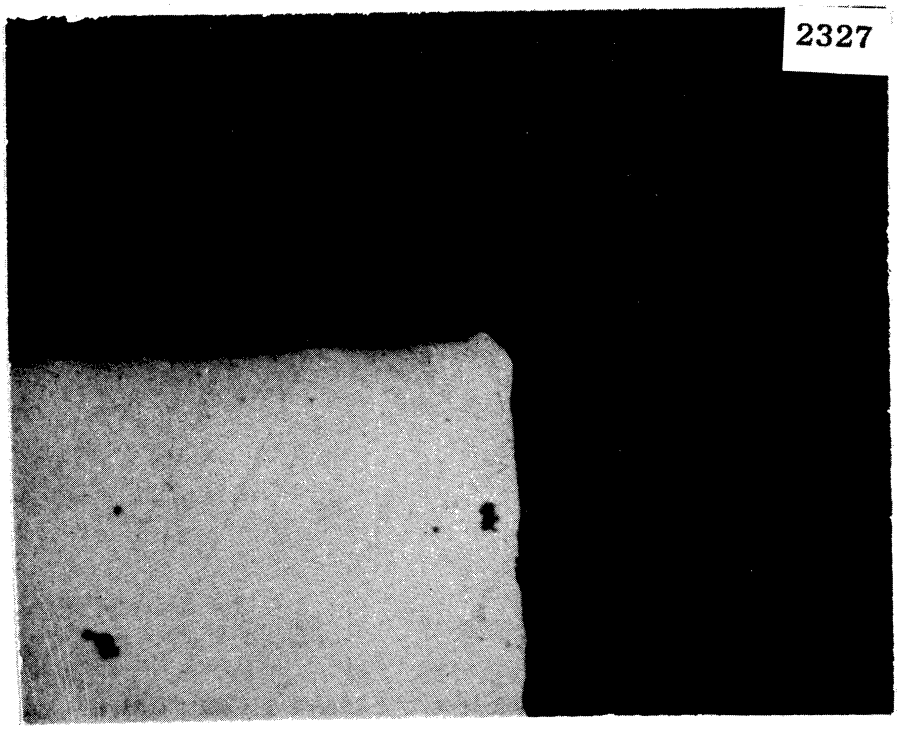

Fig. 28.--Photomicrograph of corner of specimen #Ni-168 (nickel, 1600°F anneal, 1 hour) after 100 hours exposure to "standard cavitation" in water (80°F) at a throat velocity of 200 feet per second. Magnification 250X. Unetched specimen.

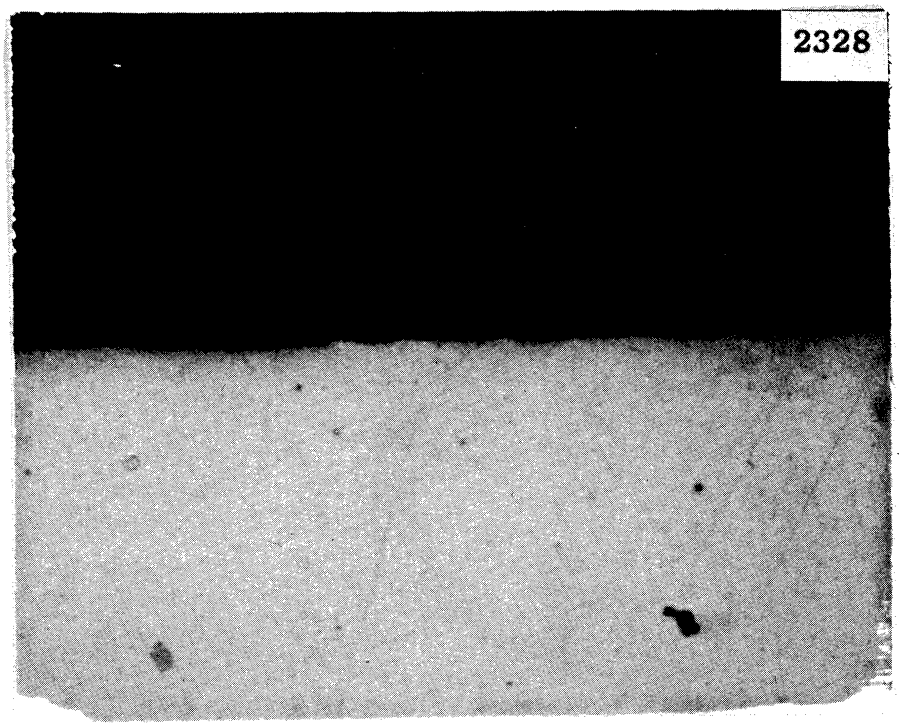

Fig. 29.--Photomicrograph of surface of specimen #Ni-168 (nickel, 1600°F, 1 hour) after 100 hours exposure to "standard cavitation" in water (80°F) at a throat velocity of 200 feet per second. Magnification 250X. Unetched specimen.

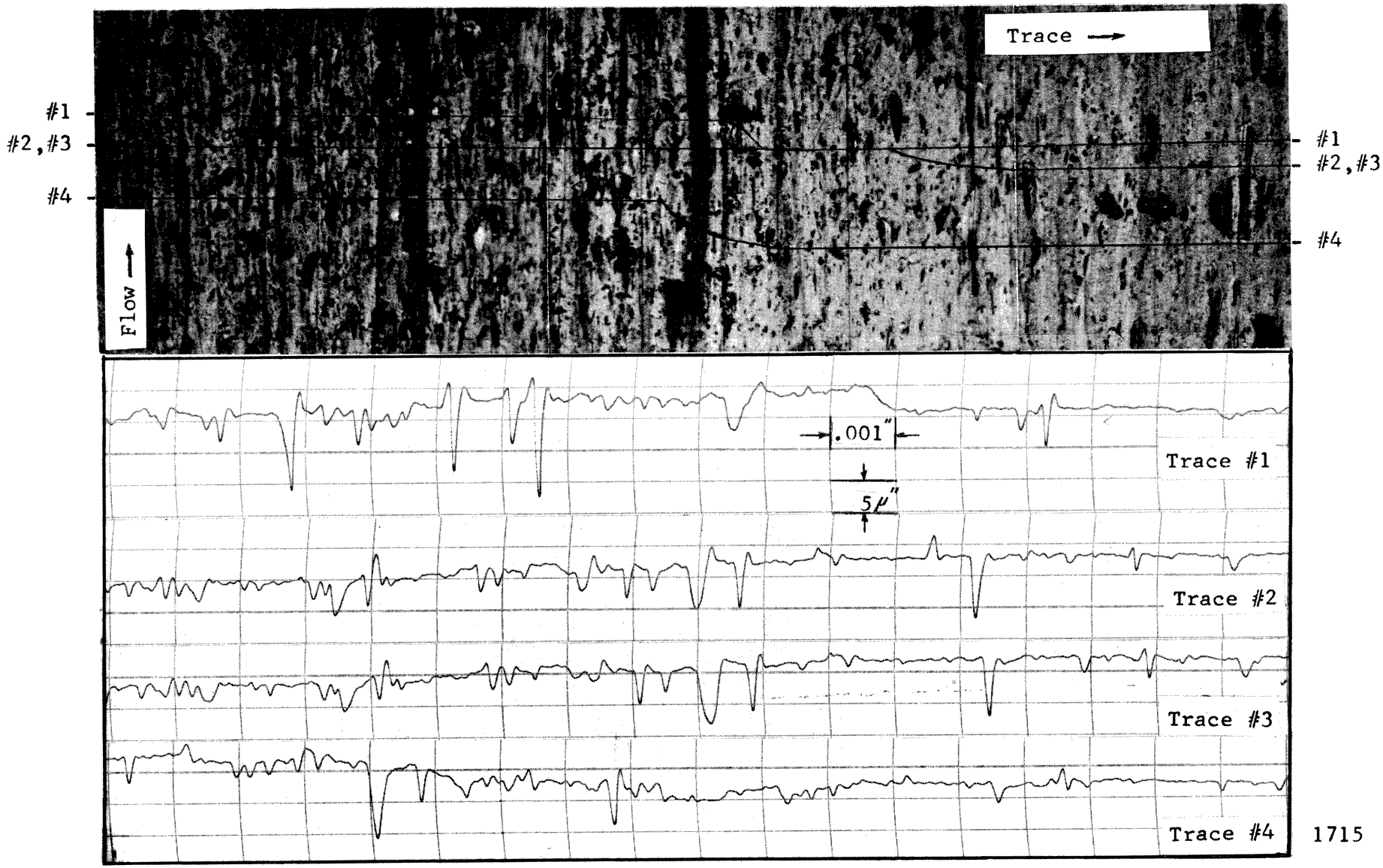

Fig. 30.--Typical photomicrographs and corresponding transverse proficorder traces of cavitated surface of specimen #Cu-Ni-8 (copper-nickel alloy, 60% cold-worked) after 100 hours in water at a throat velocity of 200 feet per second for "standard cavitation."

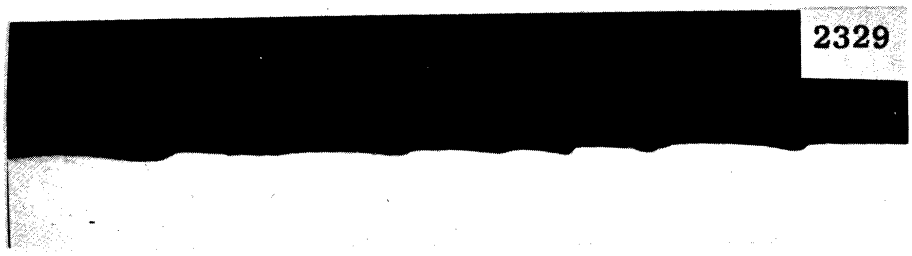

(a)

(b)

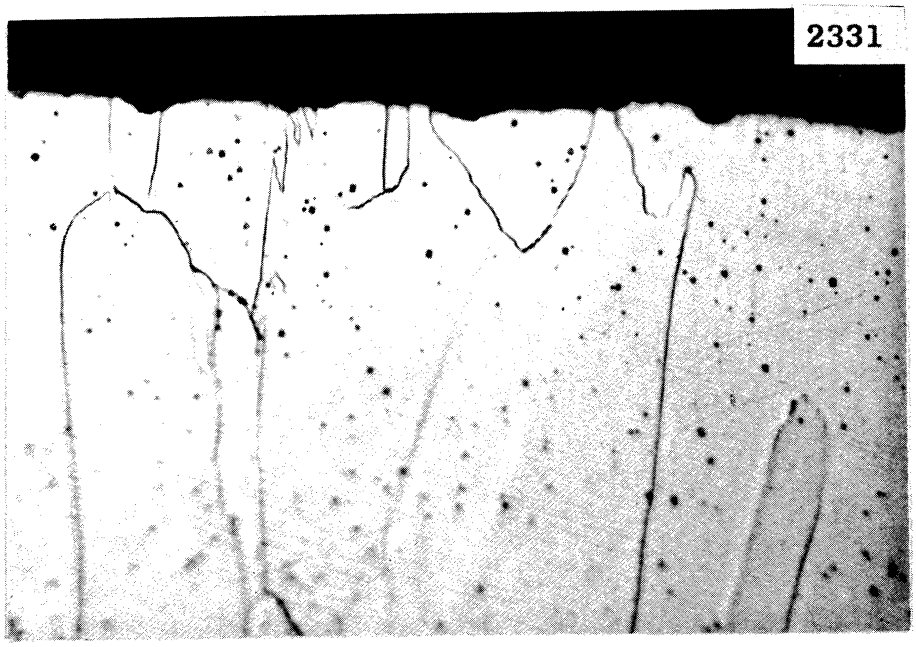

(c)

Fig. 31.--Photomicrographs of surface of specimen #Ni-13 (nickel, 75% cold-worked) after exposure to cavitation in mercury. Magnification 1000X. (a) Unetched, (b) Unetched, (c) Etched.

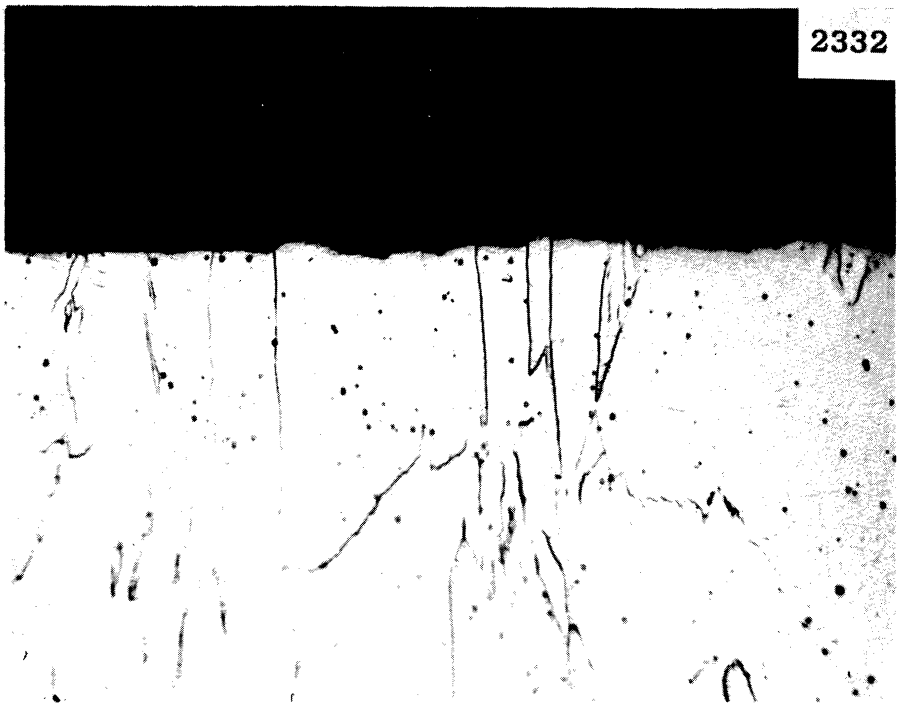

(a)

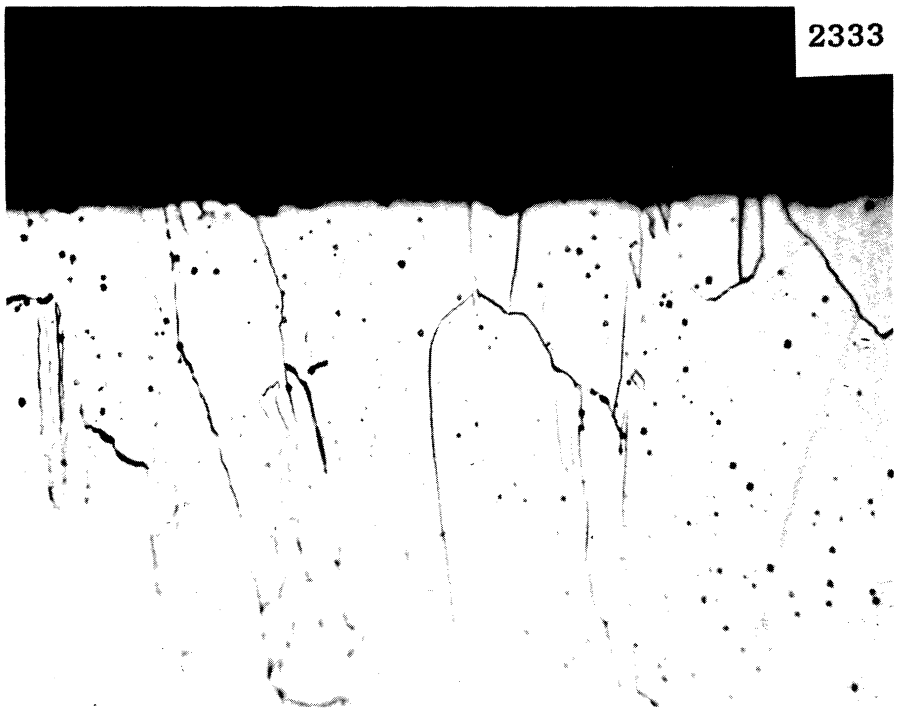

(b)

Fig. 32.--Photomicrographs of surface of specimen #Ni-13 (nickel, 75% cold-worked) after exposure to cavitation in mercury. Magnification 1000X. (a) Etched, (b) Etched.

(a)

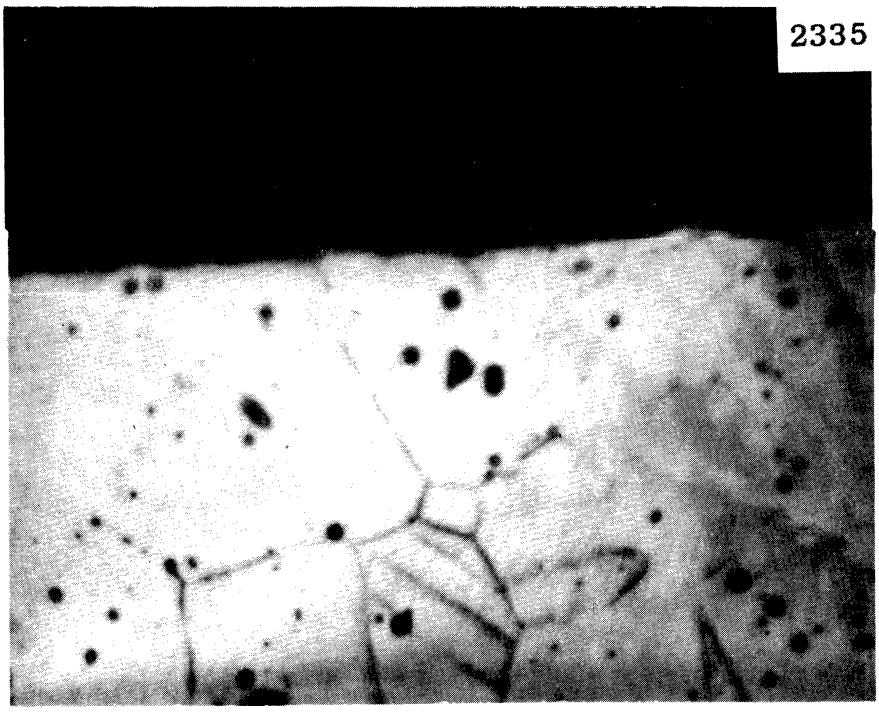

(b)

Fig. 33.--Photomicrographs of surface of specimen #SS-23 (stainless steel) after exposure to cavitation in mercury. Magnification 1000X. (a) Unetched, (b) Etched.

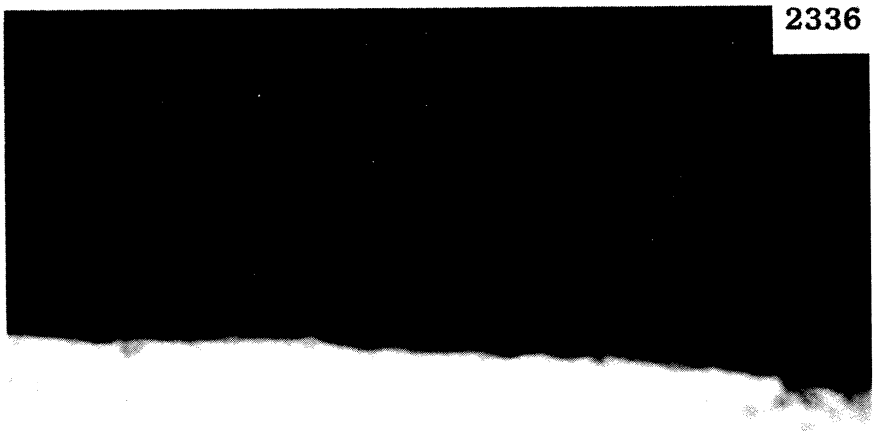

(a)

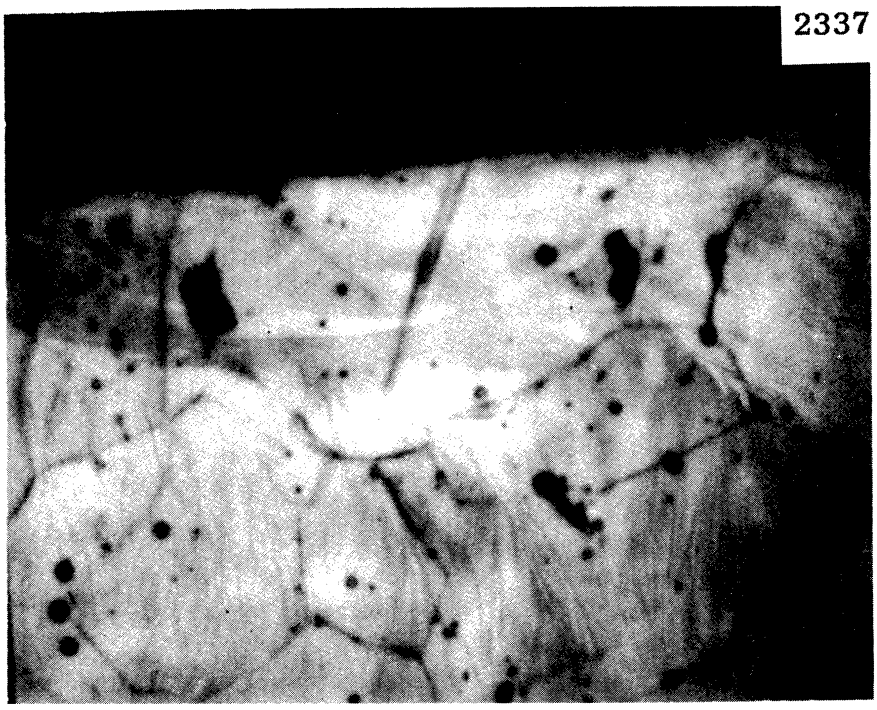

(b)

Fig. 34.--Photomicrographs of surface of specimen #SS-23 (stainless steel) after exposure to cavitation in mercury. Magnification 1000X. (a) Unetched, (b) Etched.

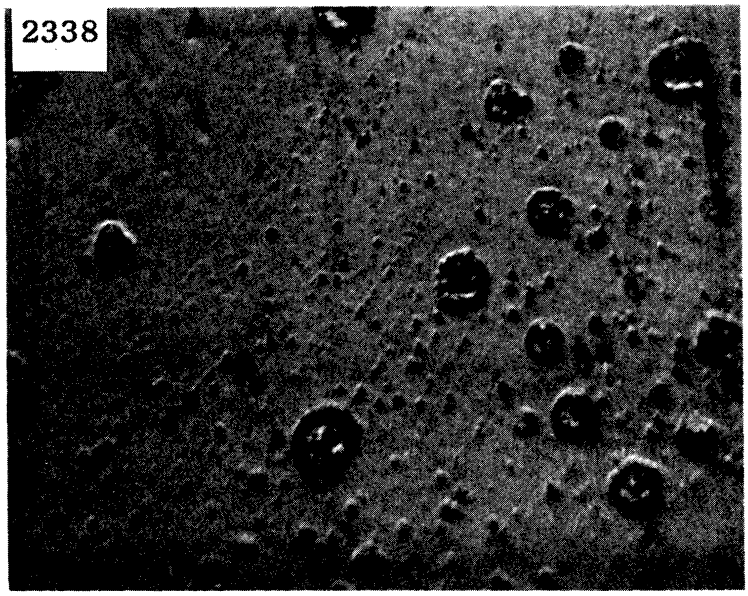

Fig. 35.--Photomicrograph of surface of specimen #P-6 (plexiglas) after exposure to "standard cavitation" in water at a throat velocity of 200 feet per second. Magnification 500X.

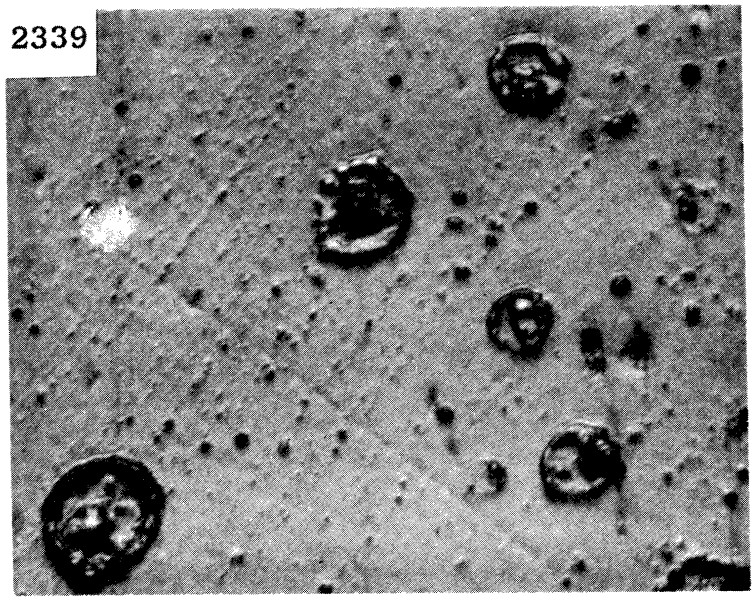

Fig. 36.--Photomicrograph of surface of specimen #P-6 (plexiglas) after exposure to "standard cavitation" in water at a throat velocity of 200 feet per second. Magnification 1000X.

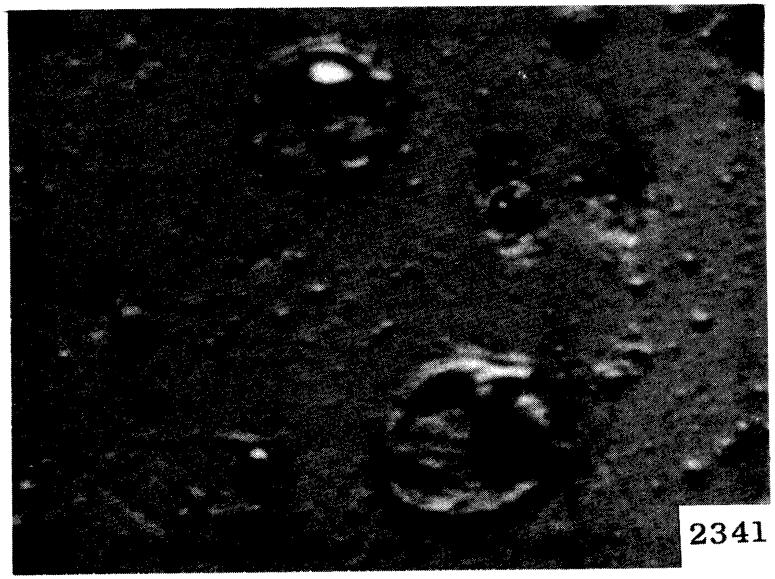

(b)

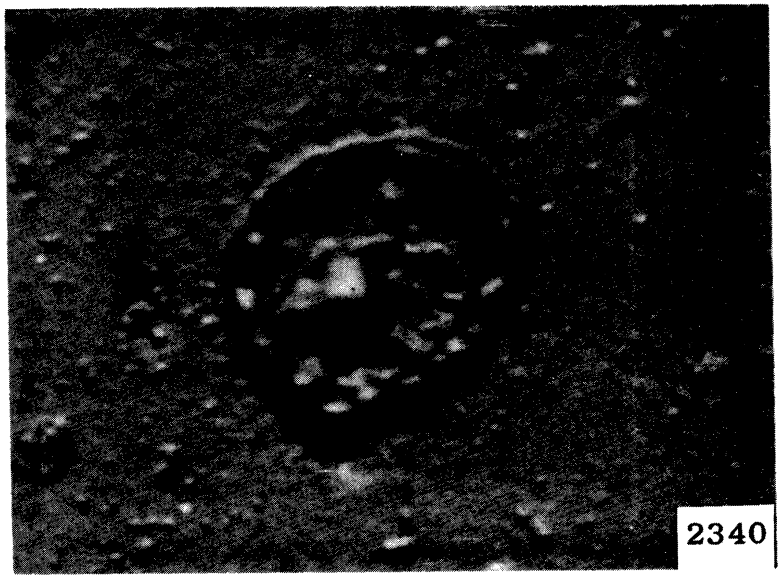

(a)

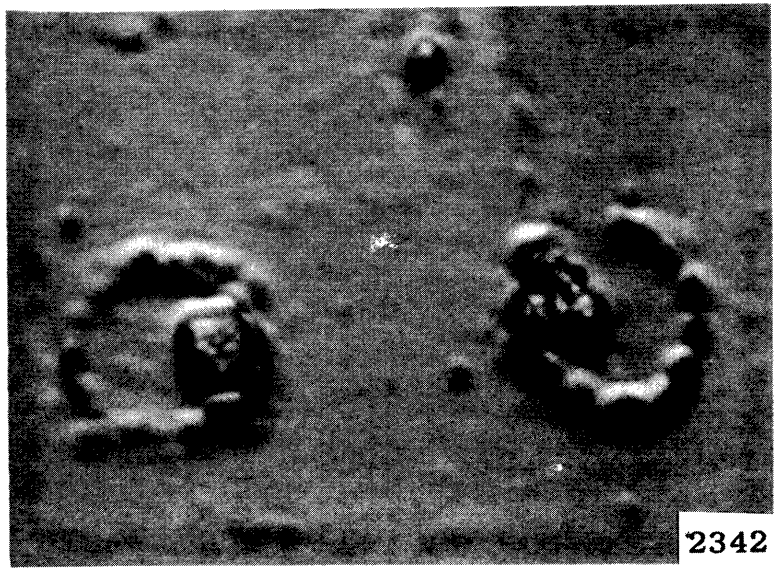

(c)

Fig. 37.--Photomicrographs of surface of specimen #P-6 (plexiglas) after exposure to "standard cavitation" in water at a throat velocity of 200 feet per second. Magnification 2000X.

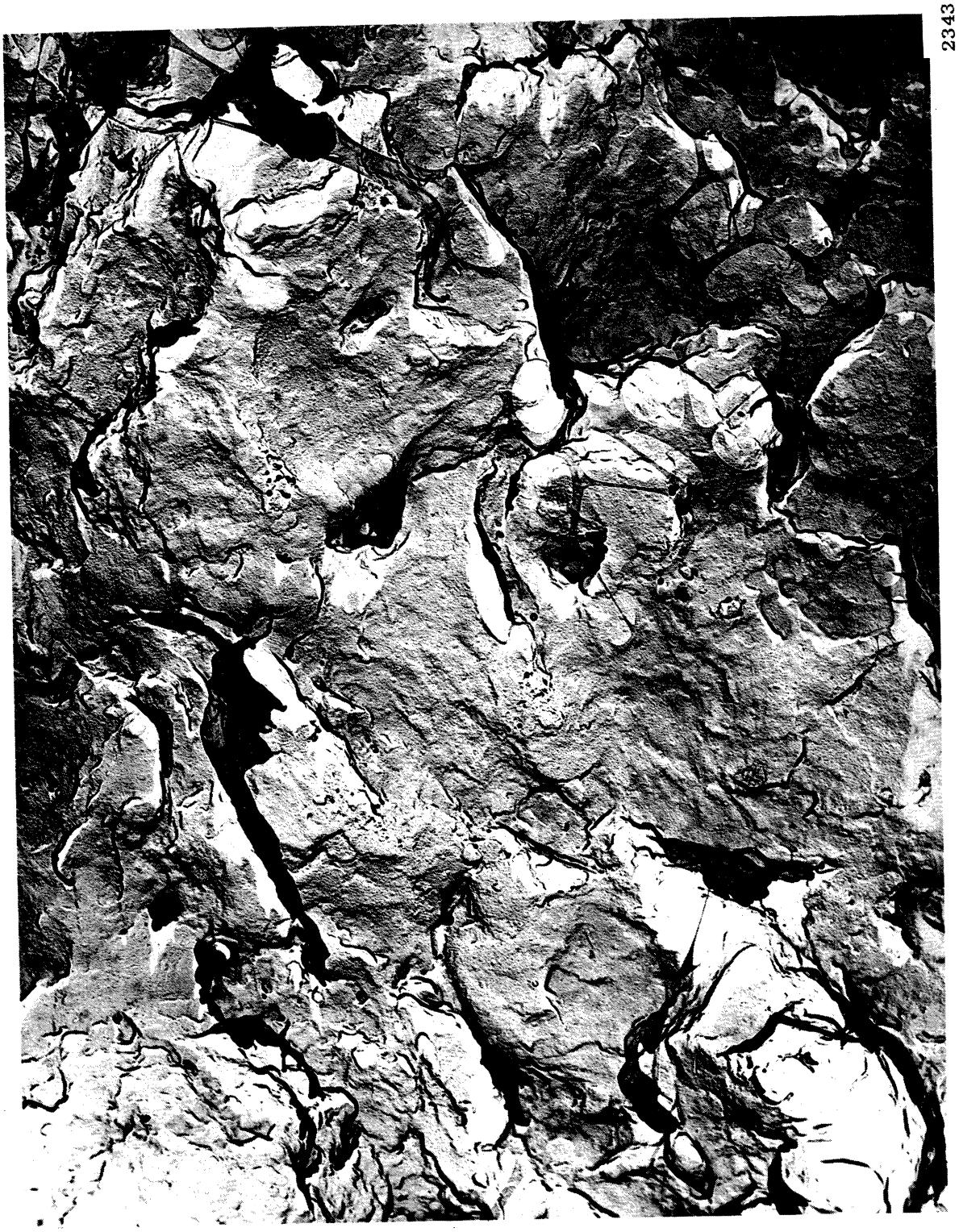

Fig. 38.--Electron photomicrograph of surface of type 304 stainless steel specimen subjected to cavitation damage in mercury for 1 hour in the ultrasonic facility. Magnification 60,000X.

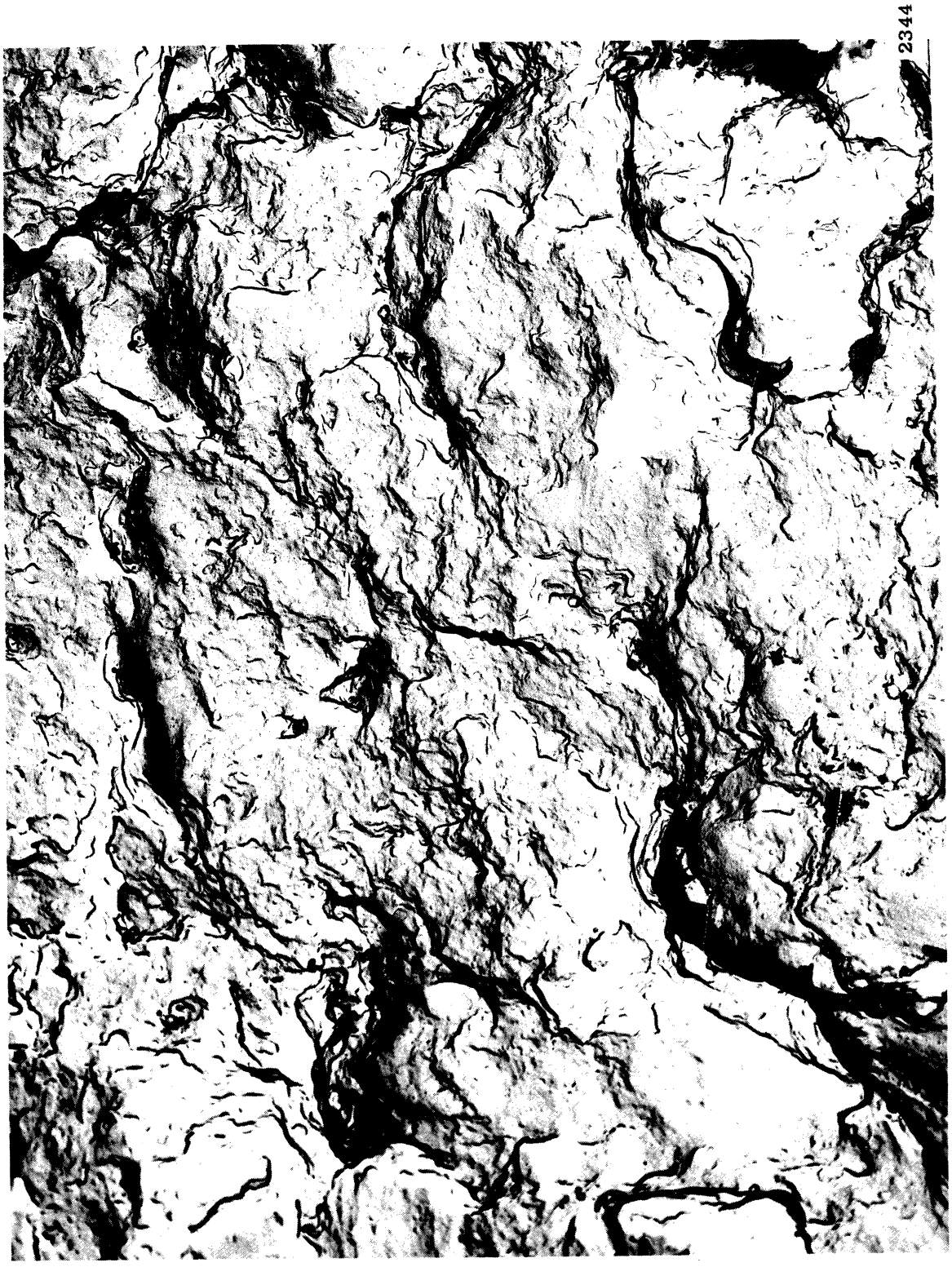

Fig. 39.--Electron photomicrograph of surface of type 304 stainless steel specimen subjected to cavitation damage in mercury for 1 hour in the ultrasonic facility. Magnification 60,000X.

Fig. 40.--Electron photomicrograph of surface of type 304 stainless steel specimen subjected to cavitation damage in mercury for 1 hour in the ultrasonic facility. Magnification 60,000X.

Fig. 41.--Electron photomicrograph of surface of type 304 stainless steel specimen subjected to cavitation damage in mercury for 1 hour in the ultrasonic facility. Magnification 60,000X.

APPENDIX

DEFINITIONS OF CAVITATION CONDITIONS

The degree of cavitation as defined in the overall damage investigations in this laboratory and in this particular investigation differ between mercury and water. In the mercury venturi, where only two specimens are used, cavitation initiates at the throat outlet for all velocities used thus far, and the degree of cavitation applied to the mercury tests describes the extent of the cavitation cloud starting at the throat outlet and extending downstream to the point indicated, i.e., "cavitation to nose" is self-explanatory. However, in the case of water, where three specimens are used, thus presenting more blockage to the venturi, the cavitation cloud initiates on the nose of the specimens and extends downstream to some point arbitrarily labeled by the degree of cavitation terminology. The first visible manifestation of cavitation occurs on the nose of the test specimen, and thus the term "visible initiation" was applied in this case. Then, succeeding degrees of more fully developed cavitation followed the old progression, regardless of the termination point on the specimen. The following are the definitions of the degrees of cavitation as used in this investigation:

Mercury

Visible Initiation	-	continuous ring of cavitation at the throat outlet, about 1/8" long.
Cavitation to Nose	-	cavitation cloud extends from throat outlet to termination at the nose of the specimen.

Standard Cavitation - cavitation cloud extends from throat outlet to termination at the middle of the specimen.

Cavitation to Back - cavitation cloud extends from throat outlet to termination at the rear of the specimen.

Water

Visible Initiation - cavitation cloud extends from nose of specimen to a point downstream on specimen about 1/8" long.

Cavitation to Nose - cavitation cloud extends from nose of specimen to termination at the middle of the specimen.

Standard Cavitation - cavitation cloud extends from nose of specimen to termination at the rear of the specimen.

From the pressure profile data in reference 3, the correspondence between water and mercury from a standpoint of degree of cavitation is as follows:

Mercury Condition (2 spec.)	corresponds to	Water Condition (3 spec.)
Cavitation to Nose	--	Visible Initiation
Standard Cavitation	--	Cavitation to Nose
Cavitation to Back	--	Standard Cavitation

This would result in the pressure gradients on the surfaces and the termination points on the surfaces being approximately the same for corresponding conditions from water to mercury.

REFERENCES

1. Hammitt, F. G., Barinka, L. L., Biss, V. A., Ivany, R. D., Pehlke, R. D., Robinson, M. J., and Siebert, C. A., "Cavitation Damage in Mercury and Water in a Cavitating Venturi and Other Components," ORA Technical Report No. 03424-9-T, Department of Nuclear Engineering, The University of Michigan, September, 1963.

2. Hammitt, F. G., Robinson, M. John, Siebert, C. A., and Aydinmakine, F. A., "Cavitation Damage Correlations for Various Fluid-Material Combinations," ORA Technical Report No. 03424-14-T, Department of Nuclear Engineering, The University of Michigan, October, 1964.

3. Robinson, M. John, "On the Detailed Flow Structure and the Corresponding Damage to Test Specimens in a Cavitating Venturi," Ph.D. Thesis and ORA Technical Report No. 03424-16-T, Department of Nuclear Engineering, The University of Michigan, August, 1965.

4. Robinson, M. J., and Hammitt, F. G., "Cavitation Damage Characteristics in Water and Mercury from Studies in a Cavitating Venturi," ORA Technical Report No. 03424-17-T, Department of Nuclear Engineering, The University of Michigan, April, 1966.

5. Garcia, R., "Comprehensive Cavitation Damage Data for Water and Various Liquid Metals Including Correlations with Material and Fluid Properties," Ph.D. Thesis and ORA Technical Report No. 05031-6-T, Department of Nuclear Engineering, The University of Michigan, August, 1966.

6. Hammitt, F. G., "Cavitation Damage and Performance Research Facilities," Symposium on Cavitation Research Facilities and Techniques, pp. 175-184, ASME Fluids Engineering Division, May, 1964. See also ORA Technical Report No. 03424-12-T, Department of Nuclear Engineering, The University of Michigan, November, 1963.

7. Personal Communication from J. W. Holl, Ordnance Research Laboratory, Pennsylvania State University, University Park, Pennsylvania.

8. Bowden, F. P., and Brunton, J. H., "The Deformation of Solids by Liquid Impact at Supersonic Speeds," Proc. of the Royal Society, A, Vol. 263, pp. 433-450, 1961.

9. Hobbs, J. M., "Experience with a 20-Kc. Cavitation Erosion Test," Paper #120 presented at 1966 Annual ASTM Meeting, Symposium on Erosion by Cavitation or Impingement, Atlantic City, New Jersey, June, 1966; to be published by ASTM.